Research Square

Preprints are preliminary reports that have not undergone peer review.
They should not be considered conclusive, used to inform clinical practice,
or referenced by the media as validated information.

Thermal acclimation dampens the warming-induced increase in ecosystem respiration

Junna Wang
junna.wang@yale.edu
Yale University

David Reed
david.e.reed@yale.edu
Yale University

Aimee Classen
aclassen@umich.edu
University of Michigan https://orcid.org/0000-0002-6741-3470

Alexander Knohl
aknohl@uni-goettingen.de
University of Goettingen https://orcid.org/0000-0002-7615-8870

Andrej Varlagin
varlagin@sevin.ru
A.N. Severtsov Institute of Ecology and Evolution, Russian Academy of Sciences
https://orcid.org/0000-0002-2549-5236

Andrew Ouimette
Andrew.Ouimette@usda.gov
U. S. Dept. of Agriculture, Forest Service

Ankur Desai
desai@aos.wisc.edu
University of Wisconsin-Madison https://orcid.org/0000-0002-5226-6041

Bernard Heinesch
bernard.heinesch@ulg.ac.be
Department of Biosystem Engineering (BioSE), Gembloux Agro-Bio Tech, University of Liege

Chad Hanson
chad.hanson@oregonstate.edu
Oregon State University

Christopher Gough
cmgough@vcu.edu
VCU https://orcid.org/0000-0002-1227-7731

Christopher Still
chris.still@oregonstate.edu
Oregon State University https://orcid.org/0000-0002-8295-4494

Damien Bonal
damien.bonal@inrae.fr

INRAE https://orcid.org/0000-0001-9602-8603

Dan Yakir
dan.yakir@weizmann.ac.il
Weizmann Institute of Science https://orcid.org/0000-0003-3381-1398

Dennis Baldocchi
baldocchi@berkeley.edu
University of California, Berkeley https://orcid.org/0000-0003-3496-4919

Eeva-Stiina Tuittila
eeva-stiina.tuittila@uef.fi
University of Eastern Finland https://orcid.org/0000-0001-8861-3167

Enrique Sanchez-Cañete
enripsc@ugr.es
University of Granada

Enrique Vivoni
vivoni@asu.edu
School of Sustainable Engineering and the Built Environment, Arizona State University

Eugenie Euskirchen
seeuskirchen@alaska.edu
University of Alaska Fairbanks https://orcid.org/0000-0002-0848-4295

Giovanni Manca
Giovanni.MANCA@ec.europa.eu
European Commission https://orcid.org/0000-0002-9376-0310

Gregory Starr
gstarr@ua.edu
University of Alabama, Tuscaloosa

Guillaume Simioni
guillaume.simioni@inrae.fr
URFM, INRAE

Jean-Marc Limousin
Jean-marc.LIMOUSIN@cefe.cnrs.fr
Centre d'Ecologie Fonctionelle et Evolutive

Jeffrey Wood
woodjd@missouri.edu
University of Missouri https://orcid.org/0000-0001-6422-2882

Jiquan Chen
jqchen@msu.edu
Michigan State University https://orcid.org/0000-0003-0761-9458

Jiří Dušek
dusek.j@czechglobe.cz
Global Change Research Institute of the Czech Academy of Sciences https://orcid.org/0000-0001-6119-0838

Ladislav Šigut
sigut.l@czechglobe.cz

Department of Matter and Energy Fluxes, Global Change Research Institute of the Czech Academy of Sciences https://orcid.org/0000-0003-1951-4100

Leonardo Montagnani
leonardo.montagnani@unibz.it
Free University of Bolzano https://orcid.org/0000-0003-2957-9071

Lianhong Gu
lianhong-gu@ornl.gov
Oak Ridge National Laboratory

Altaf Arain
arainm@mcmaster.ca
https://orcid.org/0000-0002-1433-5173

Marion Bret-Harte
msbretharte@alaska.edu
University of Alaska Fairbanks https://orcid.org/0000-0001-5151-3947

Marius Schmidt
ma.schmidt@fz-juelich.de
Jülich Research Centre https://orcid.org/0000-0001-5292-7092

Masahito Ueyama
miyabi-flux@muh.biglobe.ne.jp
Osaka Metropolitan University

Matthias Peichl
matthias.peichl@slu.se
Swedish University of Agricultural Sciences https://orcid.org/0000-0002-9940-5846

Mirco Rodeghiero
mirco.rodeghiero@unitn.it
University of Trento

Nicolas Delpierre
nicolas.delpierre@universite-paris-saclay.fr
Université Paris-Saclay https://orcid.org/0000-0003-0906-9402

Nina Buchmann
nina.buchmann@usys.ethz.ch
ETH Zurich https://orcid.org/0000-0003-0826-2980

Peter Blanken
blanken@colorado.edu
University of Colorado https://orcid.org/0000-0002-7405-2220

Ralf Staebler
ralf.staebler@ec.gc.ca
Environment Canada

Sparkle Malone
sparkle.malone@yale.edu
Yale University

Physical Sciences - Article

Keywords: terrestrial carbon sinks, carbon-climate feedback, thermal adaptation, eddy covariance, FLUXNET

Posted Date: January 10th, 2025

DOI: https://doi.org/10.21203/rs.3.rs-5718150/v1

License: This work is licensed under a Creative Commons Attribution 4.0 International License.
Read Full License

Additional Declarations: There is **NO** Competing Interest.

Thermal acclimation dampens the warming-induced increase in ecosystem respiration

Junna Wang[1], David E. Reed[1], Aimee T. Classen[2,3], Alexander Knohl[4,5], Andrej Varlagin[6], Andrew Ouimette[7], Ankur R. Desai[8], Bernard Heinesch[9], Chad V. Hanson[10], Christopher M. Gough[11], Christopher Still[12], Damien Bonal[13], Dan Yakir[14], Dennis Baldocchi[15], Eeva-Stiina Tuittila[16], Enrique P. Sanchez-Cañete[17,18], Enrique Vivoni[19,20], Eugenie Euskirchen[21], Giovanni Manca[22], Gregory Starr[23], Guillaume Simioni[24], Jean-Marc Limousin[25], Jeffrey Wood[26], Jiquan Chen[27], Jiří Dušek[28], Ladislav Sigut[28], Leonardo Montagnani[29], Lianhong Gu[30], M. Altaf Arain[31], M. Syndonia Bret-Harte[21], Marius Schmidt[32], Masahito Ueyama[33], Matthias Peichl[34], Mirco Rodeghiero[35], Nicolas Delpierre[36], Nina Buchmann[37], Peter D. Blanken[38], Ralf M. Staebler[39], Sparkle L. Malone[1,40]

[1] Yale School of the Environment, Yale University, New Haven, CT, USA

[2] The University of Michigan Biological Station, Pellston, MI, USA

[3] Department of Ecology and Evolutionary Biology, University of Michigan, Ann Arbor, MI, USA

[4] Bioclimatology, Faculty of Forest Sciences, University of Göttingen, Göttingen, Germany

[5] Centre of Biodiversity and Sustainable Land Use (CBL), University of Göttingen, Göttingen, Germany

[6] A.N. Severtsov Institute of Ecology and Evolution, Moscow, Russia

[7] U. S. Dept. of Agriculture, Forest Service, Northern Research Station, Durham, NH, USA

[8] Department of Atmospheric and Oceanic Sciences, University of Wisconsin – Madison, Madison, WI, USA

[9] BIODYNE Biosystems Dynamics and Exchanges, TERRA Teaching and Research Center, Gembloux Agro-Bio Tech, University of Liege, Belgium

[10] Forest Ecosystems and Society, Oregon State University, Corvallis, OR, USA

[11] Department of Biology, Virginia Commonwealth University, Richmond, VA, USA

[12] Department of Forest Ecosystems & Society, Oregon State University, Corvallis, OR, USA

[13] AgroParisTech, INRAE, UMR Silva, Université de Lorraine, Nancy, France

[14] Department of Earth and Planetary Sciences, Weizmann Institute of Science, Rehovot, Israel

[15] Department of Environmental Science, Policy and Management, University of California, Berkeley, CA, USA

[16] School of Forest Sciences, University of Eastern Finland, Joensuu, Finland

[17] Department of Applied Physics, University of Granada, Granada, Spain

[18] Andalusian Institute for Earth System Research (CEAMA-IISTA), Granada, Spain

[19] School of Sustainable Engineering and the Built Environment, Arizona State University, Tempe, AZ, USA

[20] Center for Hydrologic Innovations, Arizona State University, Tempe, AZ, USA

[21] Institute of Arctic Biology, University of Alaska Fairbanks, Fairbanks, AK, USA

[22] European Commission, Joint Research Centre, Ispra, Italy

[23] Department of Biology, University of Alabama, Tuscaloosa, AL, USA

[24] INRAE, URFM, Avignon, France

[25] CEFE, Univ Montpellier, CNRS, EPHE, IRD, Montpellier, France

[26] School of Natural Resources, University of Missouri, Columbia, MO, USA

[27] Center for Global Change and Earth Observations, Michigan State University, East Lansing, MI, USA

[28] Global Change Research Institute of the Czech Academy of Sciences, Brno, Czech Republic

[29] Free University of Bolzano, Faculty of Agriculture, Environment and Food Sciences, Bolzano, Italy

[30] Environmental Sciences Division, Oak Ridge National Laboratory, Oak Ridge, TN, USA

[31] School of Earth, Environment and Society, McMaster University, Hamilton, Ontario, Canada

[32] Institute of Bio- and Geosciences: Agrosphere (IBG-3), Research Centre Jülich, Jülich, Germany

[33] Graduate School of Agriculture, Osaka Metropolitan University, Sakai, Osaka, Japan

[34] Department of Forest Ecology and Management, Swedish University of Agricultural Sciences (SLU), Umeå, Sweden

[35] Center Agriculture Food Environment (C3A), University of Trento, San Michele All'Adige, Trento, Italy

[36] Université Paris-Saclay, CNRS, AgroParisTech, Ecologie Systématique et Evolution, Gif-sur- Yvette, France

[37] Institute of Agricultural Sciences, ETH Zurich, Zurich, Switzerland

[38] Department of Geography, University of Colorado, Boulder, CO, USA

[39] Air Quality Processes Section, Science and Technology Branch, Environment and Climate Change Canada, Toronto, ON, Canada

[40] Yale Center for Natural Carbon Capture, Yale University, New Haven, CT, USA

Keywords: terrestrial carbon sinks, carbon-climate feedback, thermal adaptation, eddy covariance, FLUXNET

Abstract

Global warming increases ecosystem respiration (ER), creating a positive carbon-climate feedback. Thermal acclimation, the direct responses of biological communities to reduce the effects of temperature changes on respiration rates, is a critical mechanism that compensates for warming-induced ER increases and dampens this positive feedback. However, the extent and effects of this mechanism across diverse ecosystems remain unclear. By analyzing CO_2 flux data from 93 eddy covariance sites worldwide, we observed thermal acclimation at 84 % of the sites. If sustained, thermal acclimation could reduce projected warming-induced nighttime ER increases by at least 25 % across most climate zones by 2041-2060. Strong thermal acclimation is particularly evident in ecosystems at high elevation, with low-carbon-content soils, and within tundra, semi-arid, and warm-summer Mediterranean climates, supporting the hypothesis that extreme environments favor the evolution of greater acclimation potential. Moreover, ecosystems with dense vegetation and high productivity such as humid tropical and subtropical forests generally exhibit strong thermal acclimation, suggesting that regions with substantial CO_2 uptake may continue to serve as strong carbon sinks. Conversely, some ecosystems in cold continental climates show signs of enhancing thermal responses, the opposite of thermal acclimation, which could exacerbate carbon losses as climate warms. Our study underscores the widespread yet climate-specific patterns of thermal acclimation in global terrestrial ER, emphasizing the need to incorporate these patterns into Earth System Models for more accurate carbon-climate feedback projections.

Introduction

The terrestrial biosphere has absorbed approximately 30% of anthropogenic CO_2 emissions over the past two decades[1]. Future trends in global terrestrial net ecosystem productivity (NEP)—the difference between ecosystem respiration (ER) and gross primary production (GPP)—are of great concern[2], as maintaining and enhancing terrestrial carbon uptake is critical to the success of nature-based climate solutions[3]. The net terrestrial CO_2 uptake in the past century was largely attributed to enhanced GPP due to CO_2 and nitrogen fertilization increasing photosynthesis, elevated temperature reducing cold limitation at higher latitudes, and forest regrowth in the Northern Hemisphere[2,4]. However, in the 21st century, the increase in GPP is projected to slow due to diminishing fertilization effects and more frequent disturbances[5–7]. Conversely, an increase in ER is expected to accelerate with continued warming, as temperature is a primary driver of ER, and temperature responses of ER are often described as exponential[8–10]. Future increases in ER may surpass GPP in the long run, transitioning terrestrial ecosystems from net carbon sinks to net carbon sources[2,11]. The timing and extent of these shifts are contingent on the degree to which terrestrial ecosystems acclimate to climate change[12,13].

One challenge in projecting future ER is the limited understanding of how living organisms acclimate to a warming environment through biochemical, physiological, and community-level adjustments[14–16]. As biological communities acclimate to warming via altering enzymes, membrane structures, or community composition, existing temperature~ER relationships may shift downward, mitigating the warming-induced increase in ER (compensating thermal response and a negative climate feedback; Fig. 1a)[12,16]. This phenomenon, termed thermal acclimation or compensating thermal response, describes the *direct* response of biological communities to reduce the effect of a temperature change on respiration rates[17]. Conversely, existing temperature~ER relationships can shift upward with warming, amplifying the increase in ER with higher temperature (enhancing thermal response and a positive climate feedback; Fig. 1b)[18]. This enhancing response occurs when dormant microbes are activated[19], enzyme activity is enhanced[20], or warming selects for organisms with higher respiration rates or genes coding for heat-shock proteins to protect cells from thermal stress[18]. However, shifts in temperature~ER relationships are not solely due to organisms' direct responses to temperature changes (i.e., thermal response). Indirect effects

of warming, such as alterations in soil water content, photosynthesis, or the availability of labile carbon in soils and plants, can also influence ER rates, a phenomenon known as apparent thermal response. For example, warming often reduces soil water and labile carbon availability, decreasing ER in water-limited areas[21,22], thereby creating apparent thermal acclimation. Quantifying the direction (compensating vs. enhancing) and strength of thermal response requires controlling for the confounding effects of apparent thermal responses, although this is challenging at the ecosystem scale[23].

Biological communities typically acclimate to temperature changes by altering temperature sensitivities (e.g., Q_{10}; type I), adjusting basal respiration rates (type II)[16], or both[24]. Most ecosystem-scale studies have focused on spatial and temporal variations in temperature sensitivities, without accounting for changes in basal respiration that may counteract or exacerbate type I effects[25,26]. Methods that assess the combined effects of the two types, such as using change ratios of respiration at growing temperatures per degree change in temperature, offer a more comprehensive estimate of the overall strength of thermal response and its implication for future respiration[27,28]. These methods have been applied to quantify thermal response strength (*TRS*) in leaf and soil respiration but not in ER, leaving the direction and the *TRS* at the larger, more complex ecosystem scale largely unknown.

Thermal response studies have mostly been conducted separately on soil, leaf, and root respiration, generating contrasting results that cannot be easily scaled to predict ecosystem responses[12,28–31]. Compensating thermal responses (i.e., thermal acclimation) of leaf and root respiration have been widely detected in boreal, temperate, and tropical trees, as well as most biomes in Australia[27,28,32–35], with a few exceptions in grasses[36]. In contrast, both compensating and enhancing thermal responses have been reported in soil respiration. Soil incubation experiments with excess carbon substrate have found prevalent compensating thermal responses across biomes from tropical to boreal regions and in global drylands[12,31]. Cooling soil incubation experiments without substrate provision, however, have detected more evidence for enhancing thermal responses, especially in soils with high carbon-to-nitrogen ratios and those from cold climates[18,37]. Some studies have investigated the drivers of thermal response, finding that the strength of compensating responses in soil respiration can increase with mean annual air temperatures of source soils[12]. A strong compensating response has been hypothesized to occur in highly fluctuating environments or

extreme climates such as alpine and arctic ecosystems, which are thought to favor the evolution of acclimation capacity to temperature changes[38,39]. However, the evidence for this hypothesis is scant and mixed[40]. It remains unclear whether variations in *TRS* of ecosystem respiration (TRS_{ER}) align with this hypothesis or are primarily driven by mean temperature and soil properties, as observed in soil respiration.

We developed a new method to quantify TRS_{ER} using nighttime ecosystem CO_2 flux data from 93 long-term ($\geq$ 8 years) AmeriFlux, ICOS, and FLUXNET sites (1217 site-years). These sites cover various land cover classes and climates—forests, grasslands, savannas, shrublands, and wetlands in arid, semi-arid, Mediterranean, tropical, subtropical, continental, and tundra climates (Fig. 1c and Table S1). To control for apparent thermal responses via soil water pathways, we developed an ER model that includes both temperature and water content of topsoil layer (depth < 0.1 m) to capture direct temperature responses of ER. To quantify the combined effects of type I and type II thermal responses, we defined site-specific TRS_{ER} as the log-transformed change ratios of nighttime ER per degree of topsoil temperature increase, averaged across multiple growing-season temperatures (Fig. S1). Thus, compensating and enhancing thermal responses correspond to negative and positive TRS_{ER}, respectively (Fig. 1).

Here, we first present site-specific TRS_{ER} estimated by our method and its comparison with *TRS* of soil, leaf and root respiration derived from the literature. We then illustrate how TRS_{ER} varies with four representative variables, identified from 11 variables describing geographic, climatic, soil, and vegetation properties. Finally, we demonstrate the extent to which thermal response could mitigate or exacerbate future growing-season nighttime ER increases induced by warming across different climates by mid-century (2041-2060).

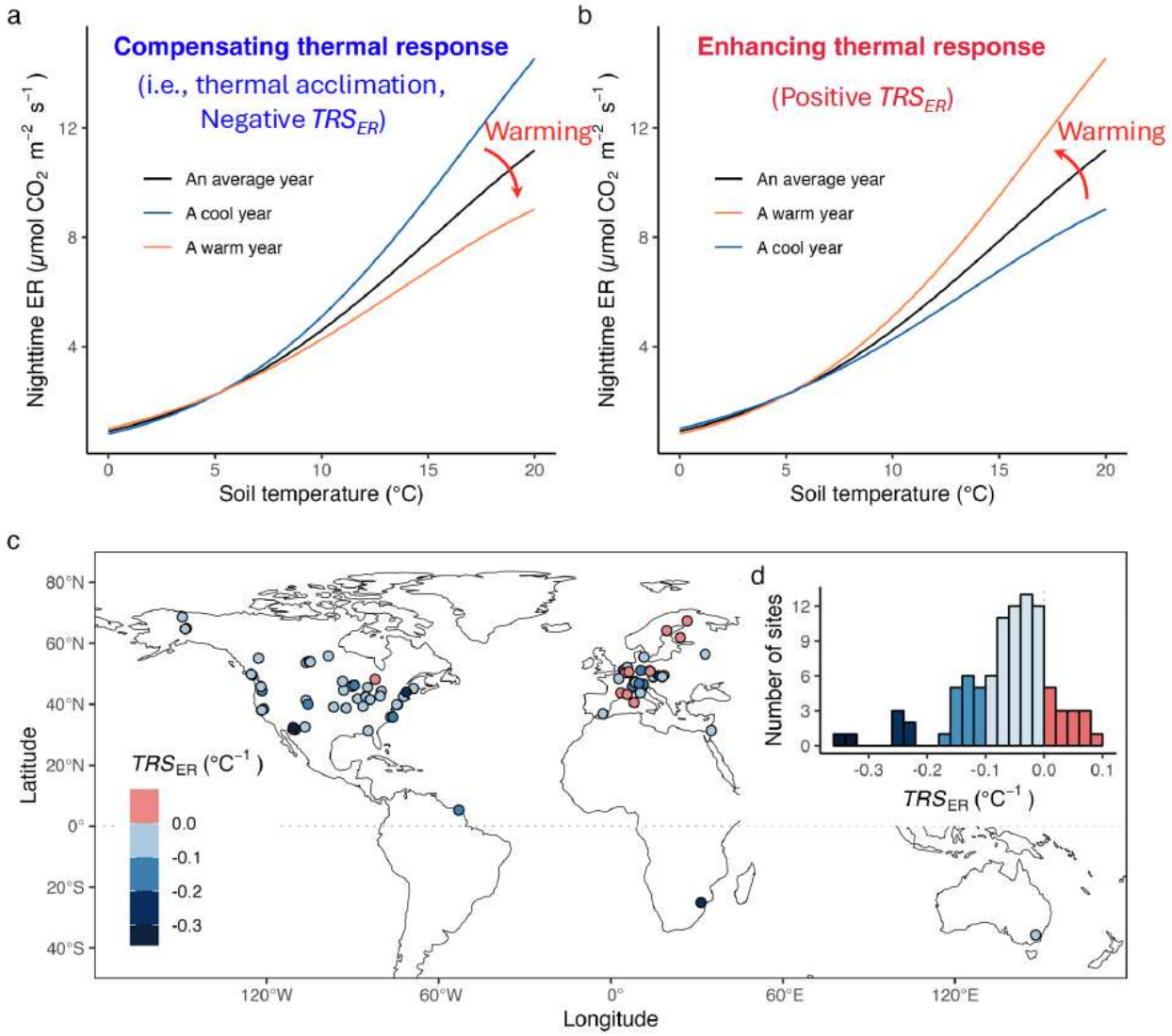

Figure 1. Conceptual illustration of compensating thermal response (i.e., thermal acclimation) (a) and enhancing thermal response (b) of nighttime ecosystem respiration (ER), the global distribution of the 93 long-term eddy covariance flux study sites (c), that show variable thermal response strength of ecosystem respiration (TRS_{ER}) (d).

Results

Compensating thermal responses dominate TRS_{ER}

We detected both compensating (negative TRS_{ER}) and enhancing (positive TRS_{ER}) thermal responses, with 84 % of study sites (78 out of 93) showing compensating thermal responses (Fig. 1d). Across sites, TRS_{ER} values ranged from -0.345 to 0.094 °C^{-1}, with a mean of -0.065 °C^{-1} (Fig. 2). At the

78 sites with negative TRS_{ER}, 31 sites (40 %) were statistically significant ($p < 0.1$; i.e., their TRS_{ER} values were negative at 90 % of confidence interval). With a small sample size, we considered $p < 0.1$ as statistically significant[41] because 70 % of sites had less than 15 years of data (Table S1), with each year contributing to one data point for calculating TRS_{ER} (Fig. S1c). The limited data duration at most sites resulted in the low fraction of sites with significant thermal responses. The percentage of sites exhibiting significant thermal responses increased with data duration, reaching 60 % for sites with more than 20 years of data (Fig. S2). In contrast to the predominate negative TRS_{ER} values, only 15 sites exhibited positive TRS_{ER}, none of which were statistically significant ($p > 0.17$; Fig. 2 and Table S1). This indicates that enhancing thermal responses at the ecosystem scale are much less common than compensating thermal responses among terrestrial ecosystems globally. Sites showing signs of enhancing thermal response were mostly distributed in latitudes above 40° and in cold continental climate (red points in Fig. 1c and Table S1).

We compared TRS_{ER} with TRS of soil, leaf, and root respiration derived from *in-situ* warming experiments and field observations in the literature. There was no significant difference between TRS_{ER} values at our sites with significant thermal acclimation ($n = 31$) and those from previous studies where significant thermal acclimation in soil, leaf, and root respiration was also detected ($n = 44$; Table S2), as indicated by an unpaired *t*-test ($t = 0.69$, $df = 71.39$, $p = 0.49$; Fig. 2). Furthermore, we found one *in-situ* soil warming experiment conducted in the same climate and vegetation class as one of our flux sites. The *TRS* of soil respiration in a tallgrass prairie[26] (–0.081 $°C^{-1}$) closely matched TRS_{ER} at a grassland flux site (US-Kon; –0.071 $°C^{-1}$; Table S1). This slightly weaker ecosystem-level TRS_{ER} (less negative) might be due to little-to-no thermal acclimation of leaf respiration observed in the same prairie[36]. These comparisons suggest that across climates, TRS_{ER} at the sites with significant thermal acclimation is comparable to *TRS* of soil, leaf and root respiration, validating the method we developed to quantify TRS_{ER}.

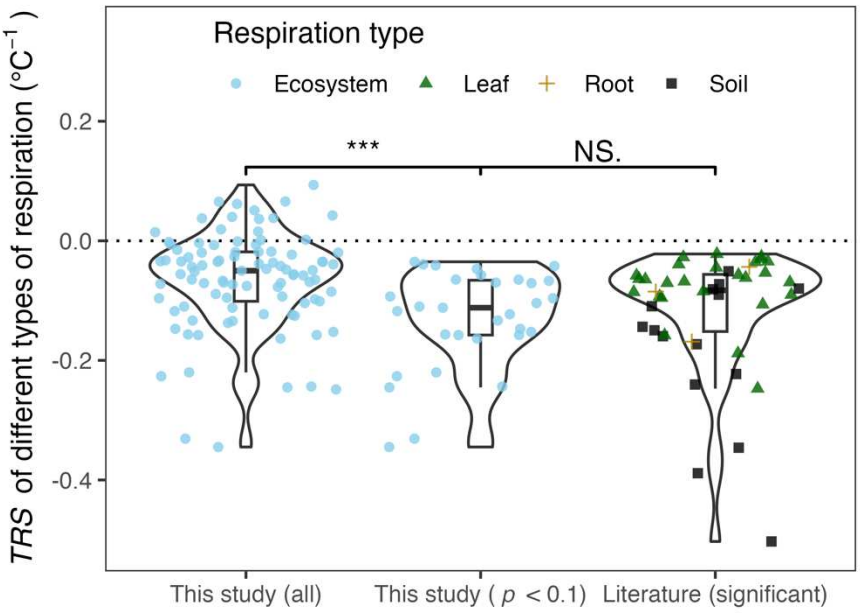

Figure 2. Comparison of thermal response strength (*TRS*) in ecosystem respiration estimated in this study across all sites ("this study (all)"; n = 93), for sites with significant thermal responses only ("this study ($p < 0.1$)"; n = 31), and *TRS* of soil, leaf, and root respiration from the literature where significant thermal acclimation was detected through *in-situ* warming experiments or field measurements ("literature (significant)", n = 44; see Table S2 for data sources). All significant thermal responses observed in this study were compensatory (*TRS* < 0, i.e., thermal acclimation). "***" denotes a statistically significant difference at the 0.001 level ($p < 0.001$), while "NS." indicates a non-significant difference ($p > 0.1$). Significant differences were tested by unpaired *t*-tests.

Extreme environments and vegetation productivity drive variations in TRS_{ER}

Across the Köppen climate classes, TRS_{ER} values differed significantly (Fig. 3a; $p < 0.1$ by analysis of variance). The strongest compensating thermal response (the most negative TRS_{ER}) was observed in the coldest climate tundra (ET), followed by tropical (Am), semi-arid (Bsh and Bsk), and warm-summer Mediterranean (Csb) climates (Fig. 3a). Conversely, the weakest compensating and even enhancing thermal responses (largest TRS_{ER}) were found in arid (Bwk) and hot-summer Mediterranean (Csa) climates. Humid subtropical (Cfa and Cfb) and continental climates (Dfa, Dfb, Dfc, Dfd, and Dwc) exhibited highly variable and overall intermediate TRS_{ER} values (Fig.

3a). Unlike the climate classes, there was no significant difference in TRS_{ER} among the International Geosphere–Biosphere Programme's (IGBP) land cover classes (Fig. S3a; $p = 0.19$ by analysis of variance). While land cover is shaped by climate[42], the same land cover class, such as open shrublands distributed in arid climate (Bwk) versus tundra climate (ET), can exhibit significantly different TRS_{ER} values (Table S1 and Figs. 3a and S3a). This suggests that climate class can have a stronger influence than land cover class in determining TRS_{ER}.

We employed random forest models to further analyze the relative importance of variables affecting TRS_{ER} and the characteristics of these relationships (e.g., linear or nonlinear). Due to strong correlations among the 11 predictor variables, especially within the same category (Table 3 and Fig. S4), we selected one variable from each category to avoid overfitting and to enhance model interpretability. We also ensured that correlation coefficients between any two selected variables were less than 0.4. Using the four selected variables—elevation (geographic), mean annual air temperature (MAT, climatic), soil organic carbon stock of the top 0.3 m soils (SOC, soil), and mean annual leaf area index (LAI, vegetation)—the random forest model explained 64 % of variation in TRS_{ER}, with elevation and LAI emerging as the two most important variables for improving model accuracy, followed by MAT and SOC (Fig. 3b).

TRS_{ER} varied with the four variables in different ways. The magnitude of compensating TRS_{ER} increased with elevation (more negative) in a nearly linear fashion, with most alpine ecosystems above 2000 m exhibiting strong, significant compensating thermal responses, as revealed by both the random forest model (Fig. 3c) and simple correlation analysis (Fig. S3b). While the magnitude of compensating TRS_{ER} also increased with LAI (more negative), a variable representing vegetation density and productivity and highly correlated with total annual precipitation (Fig. S4), the relationship was primarily threshold-type, with a marked increase in the magnitude of compensating TRS_{ER} when mean annual LAI exceeded 2.3 m^2 m^{-2} (Figs. 3d and S3c). Contrastingly, TRS_{ER} varied highly nonlinearly with MAT, with stronger compensating thermal responses observed at sites with extremely high or low MAT (Fig. 3e). This result aligns with observations of stronger compensating responses in tundra, tropical, and semi-arid climates (Fig. 3a). TRS_{ER} was less sensitive to MAT at intermediate values ranging from -2 to 20 °C. Similarly, strong compensating responses occurred at sites with

very low SOC (< 13 t ha^{-1}), above which TRS_{ER} exhibited little variation with SOC (Fig. 3f).

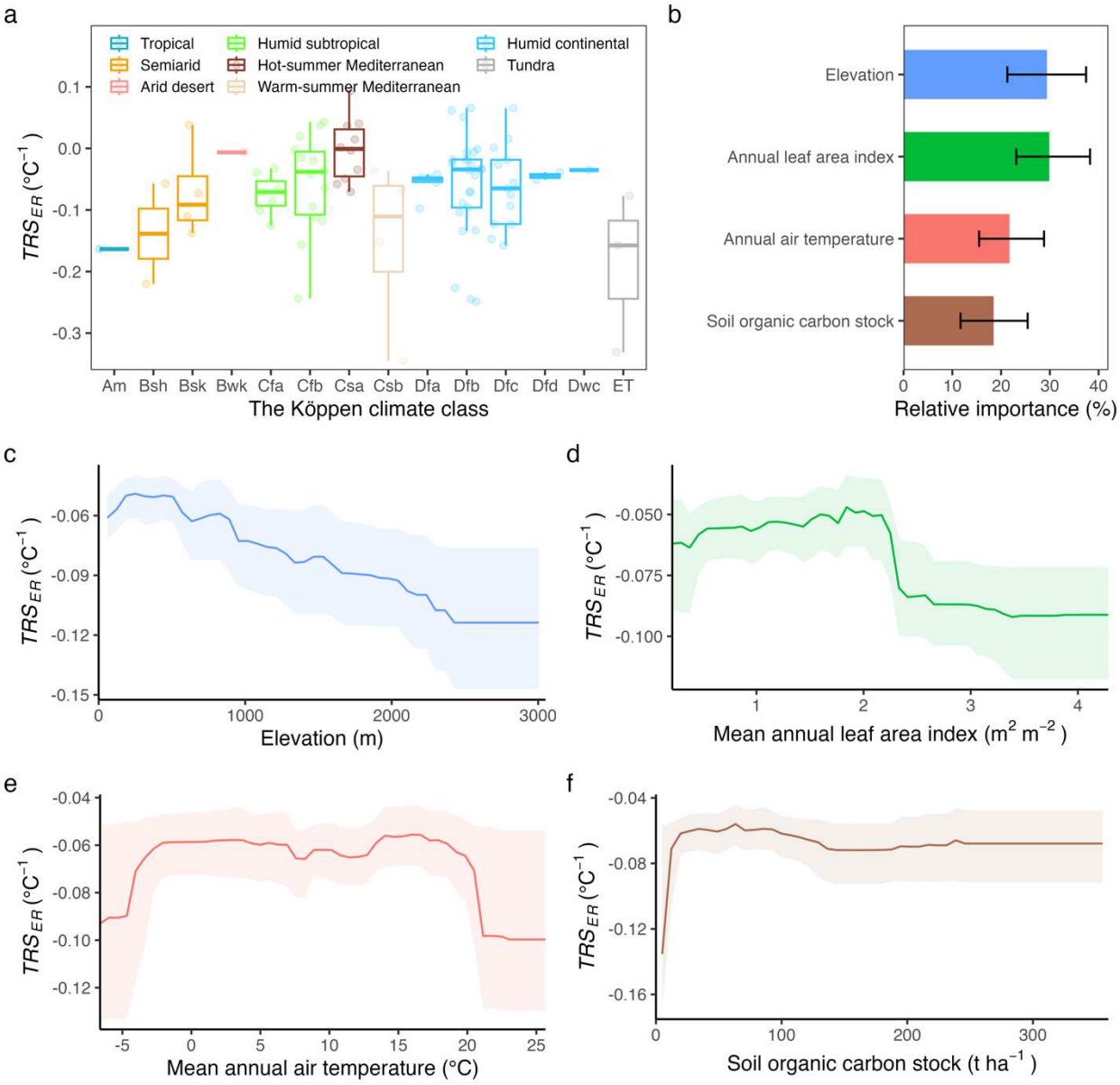

Figure 3. Variation in thermal response strength in ecosystem respiration (TRS_{ER}) across the Köppen climate classes (a), relative importance of the four representative variables for explaining TRS_{ER} variation (b), and partial dependence plots showing the variations in TRS_{ER} with the four variables (c-f). The variable soil organic carbon stock was measured in the top 0.3 m soils. The lower, middle and upper hinges of the boxplot in (a) show the first, median and third quartiles of the distribution. Whiskers in the boxplot represent the 1.5 times the interquartile range from the hinges. Error bars

in (b) and shaded areas in (c-f) denote 90 % confidence intervals. The full names of the Köppen climate classes are: Am, tropical monsoon climate; Bsh, hot semi-arid climate; Bsk, cold semi-arid climate; Bwk, cold desert climate; Cfa, humid subtropical climate; Cfb, temperate oceanic climate; Csa, hot-summer Mediterranean climate; Csb, warm-summer Mediterranean climate; Dfa, hot-summer humid continental climate; Dfb, warm-summer humid continental climate; Dfc, subarctic climate; Dfd, extremely cold subarctic climate; Dwc, monsoon-influenced subarctic climate; and ET, tundra climate.

Compensating thermal responses could mitigate one-fourth of ER increases across most climates by 2041-2060

As both TRS_{ER} and the magnitude of warming vary significantly across climate classes, the fraction of warming-induced nighttime ER increase that can be mediated by thermal responses also varied with climate classes (Figs. 4 and S5; Table S4). In tundra (ET), semi-arid (Bsh and Bsk), and warm-summer Mediterranean (Csb) climates, where strong compensating responses were observed (Fig. 3a), thermal acclimation would compensate for approximately 80 % of the future ER increase if TRS_{ER} was applied to all sites regardless of their significance levels (i.e., the “all thermal responses” scenario in Fig. 4c-d). In a more conservative estimate, if TRS_{ER} was only applied to sites with significant thermal responses and no thermal response was considered for other sites (i.e., the “significant thermal responses” scenario in Fig. 4), thermal acclimation would still compensate for 60 % of future ER increase, as all significant thermal responses were compensatory (Fig. 2). In humid tropical, subtropical, and continental climates, thermal responses would mitigate 25 % of the future increase in growing-season nighttime ER under the “significant thermal responses” scenario and 45 % under the “all thermal responses” scenario (Fig. 4e).

In contrast, in dry (Bwk) and hot-summer Mediterranean (Csa) climates, characterized by weak compensating or even enhancing thermal responses (Fig. 3a), thermal responses would not significantly limit the warming-induced ER increase (Figs. 4f and S5). Despite the weak compensating thermal responses, the overall future ER increases in these climates would be limited to 6 % of current ER rates (Fig. 4f). This limited increase primarily results from the relatively flat or the hump-shaped relationships, rather than exponential ones, between topsoil temperature (T_S) and ER in these climates (Fig. S6d-e). For sites with clear hump-shaped T_S~ER relationships, where the optimal temperatures are reached during the

growing season, the negative T_S~ER relationships beyond the optimal temperatures can significantly constrain future ER increases with warming, preventing dramatic ER increases in these hot, dry climates.

Assuming no change in land cover, the mean ER increases by 2041-2060 under the medium warming scenario (Shared Socioeconomic Pathways: SSP245) were projected to be lower than 10 % of current respiration rates in almost all climates, even under the “significant thermal responses” scenario (Fig. 4b-f; Table S4). These surprisingly low increases in ER are attributed not only to the predominant compensating thermal responses, but also the much lower increases in soil temperature compared to air temperature (Fig. 4a). Plant canopy coverage in most regions, except arid and semi-arid climates, alters the microclimate, resulting in topsoil temperature increases that are 25 ± 21 % smaller than those of air temperature (Figs. 4a and S5a). This serves as a crucial mechanism to mitigate large increases in ER, particularly soil respiration, with warming in well-vegetated areas.

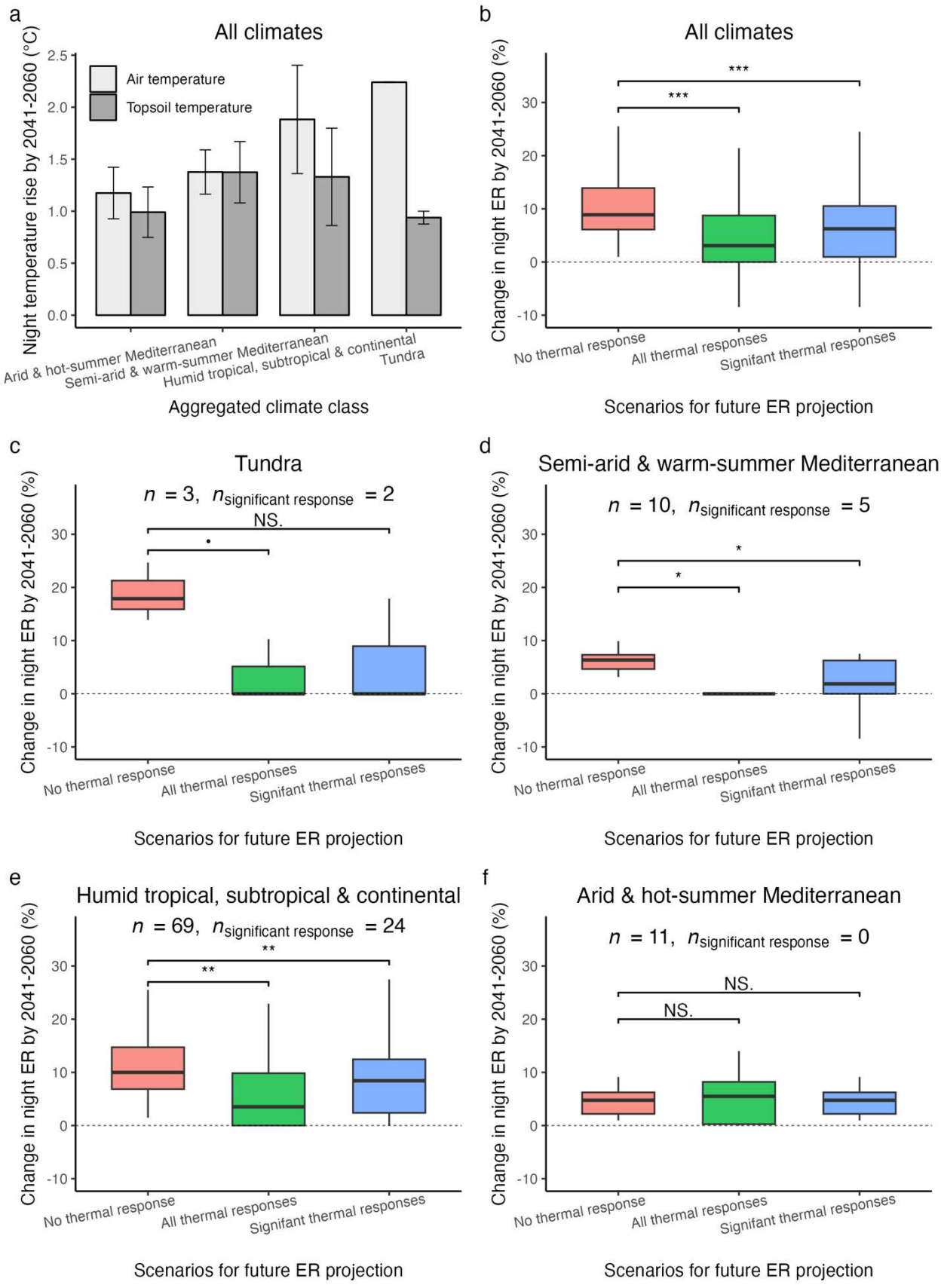
a
All climates
Night temperature rise by 2041-2060 (°C)
Air temperature
Topsoil temperature
Arid & hot-summer Mediterranean
Semi-arid & warm-summer Mediterranean
Humid tropical, subtropical & continental
Tundra
Aggregated climate class
b
All climates
Change in night ER by 2041-2060 (%)
No thermal response
All thermal responses
Signifant thermal responses
Scenarios for future ER projection
c
Tundra
n = 3, n significant response = 2
NS.
Change in night ER by 2041-2060 (%)
Scenarios for future ER projection
d
Semi-arid & warm-summer Mediterranean
n = 10, n significant response = 5
Change in night ER by 2041-2060 (%)
Scenarios for future ER projection
e
Humid tropical, subtropical & continental
n = 69, n significant response = 24
Change in night ER by 2041-2060 (%)
Scenarios for future ER projection
f
Arid & hot-summer Mediterranean
n = 11, n significant response = 0
NS.
Change in night ER by 2041-2060 (%)
Scenarios for future ER projection

373

Figure 4. Projected nighttime air and topsoil (depth < 0.1 m) temperature increases during the growing season from 2000-2020 to 2041-2060 at the study sites, grouped by aggregated climate classes (a) and corresponding changes in nighttime ecosystem respiration (ER) under three scenarios (b-f): without considering compensating or enhancing thermal responses ("no thermal response"), with estimated TRS_{ER} for all sites ("all thermal responses"), and with estimated TRS_{ER} applied only to sites with significant thermal responses and no thermal response for other sites ("significant thermal responses"). In (a), error bars represent standard deviation of temperature for sites within each aggregated climate group. In (b-f), "NS." indicates no significant difference in future ER changes between the "no thermal response" scenario and each thermal response scenario, while "•", "*", "**", and "***" denote statistical significance at the 0.1, 0.05, 0.01, and 0.001 levels, respectively. Statistical differences were tested by paired *t*-tests. In (c), no statistical difference (NS.) between the "no thermal response" scenario and "significant thermal responses" scenario in tundra climate is mainly due to low number of sites ($n = 3$). The 14 Köppen climate classes are aggregated into four climate groups here based on similarity of their thermal response features (see Fig. 3a).

Discussion

Reconciling divergent thermal response patterns in soil and leaf respiration at the ecosystem scale

Controlling for apparent thermal responses via soil water pathways and quantifying the combined effects of type I and II thermal responses, this study reveals global patterns in the direction, strength, and drivers of TRS_{ER}. These patterns align with experimental findings in soil and leaf respiration. Most sites show compensating thermal responses, consistent with the widespread compensating thermal responses reported for leaf respiration across diverse biomes and from multiple acclimation experiments on root and soil microbial respiration[12,15,27,28,32,34,43]. Strong compensating thermal responses were evident in semi-arid and warm-summer Mediterranean climates, in line with findings that soil microbial respiration adapted to ambient thermal regimes in global drylands[31]. Despite the predominance of compensating responses, we identified sites with signs of enhancing thermal responses, primarily in cold continental climates above 40° latitude. Similarly, a soil cooling experiment using soils sampled from 20 global sites, 16 of which were above 40° latitude, found

more sites with enhancing rather than compensating thermal responses, particularly in cold soils[44]. By including a broader range of global ecosystems, covering diverse climates and larger geographical areas, our study reconciles the seemingly conflicting findings in soil and leaf respiration (compensating vs. enhancing dominated), as we uncover the climate-specific variations in the direction and strength of ecosystem-level thermal responses.

In cold climates except tundra, TRS_{ER} was mostly at an intermediate level or showing enhancing responses, which differs from studies finding stronger warming-induced declines in temperature sensitivity of ER (type I thermal responses towards compensating responses) in colder climates[25]. This discrepancy may result from warming-induced increases in basal respiration in non-growing season (type II thermal responses but in the opposite direction), a phenomenon observed in leaf and soil respiration[24,36]. Therefore, focusing solely on one type of thermal responses may lead to misleading conclusions about overall TRS_{ER}. While we controlled for apparent thermal responses associated with soil water pathways, we did not control for those through photosynthesis and labile soil carbon. To assess the potential influence of the photosynthesis pathway, we explored whether higher growing-season temperatures in warm years directly reduced photosynthesis. Specifically, we calculated correlations between annual mean growing season T_S and daytime primary productivity (using daytime NEP as a proxy) across ecosystems showing compensating thermal responses ($n = 78$), excluding those in arid and semi-arid climates, where photosynthesis was likely affected by warming via water pathways ($n = 6$). Significant negative correlations ($p < 0.1$) between T_S and daytime productivity were found in only 8 of the 72 ecosystems, implying that warming might not strongly decrease photosynthesis. Similarly, no significant positive correlations between T_S and daytime productivity were detected at the 15 ecosystems showing enhancing responses. Assessing apparent thermal responses via labile carbon pathways was not feasible due to a lack of data on labile soil and plant carbon at most sites. While our method for estimating TRS_{ER} cannot fully separate true thermal responses from apparent ones[45], our estimates should reflect the strength of thermal responses under current ecosystem conditions.

Mechanisms underlying drivers of TRS_{ER}

An emerging pattern in TRS_{ER} drivers shows strong compensating thermal responses are typically observed in high-elevation ecosystems, low-organic-

carbon soils, tundra, semi-arid, and warm-summer Mediterranean climates, where environments are extreme at least seasonally. This pattern supports the evolutionary hypothesis that species with strong tolerance or acclimation ability are selected by stressful environments[38,39,46]. Extreme environments often contain multiple stressors, such as low water, carbon, and nutrient contents, extreme temperature and wind conditions[47]. Organisms in these environments have likely evolved phenotypic plasticity and stress genes that help maintain relatively stable respiration rates, enabling them to cope with highly fluctuating or stressful environments[39,48,49]. In addition to true thermal acclimation, apparent ones such as decreased leaf respiration rates due to resource limitation in warmer years might also contributed to this pattern[50]. However, unlike other extreme climates, TRS_{ER} in arid and the hot-summer Mediterranean climates is particularly weak. This weak TRS_{ER} co-occurs with relatively flat or hump-shaped T_S~ER relationships (Fig. S6d-e), suggesting organisms are either water-limited, or have evolved other mechanisms to reduce respiration in hot and dry environments, such as reduced growth efficiency or enzyme activity, dormancy, or alternative metabolic pathway that respire less[51–53]. Together, thermal acclimation, hump-shaped T_S~ER relationships, and resource limitation each play crucial roles in constraining the surge of ER with warming in extreme environments.

Beyond extreme environments, stronger compensating thermal responses tend to occur in regions with dense vegetation and high primary productivity (e.g., mean annual LAI > 2.3 m^2 m^{-2}) and high annual precipitation, such as humid tropical and subtropical forests[54]. This finding aligns with the strong compensating thermal responses observed in leaf respiration of tropical trees and in tropical soils[12,55,56]. Globally, compensating thermal responses have been more consistently observed in leaf respiration than in soil respiration[18,28,37,57]. In biomes with high LAI, leaf respiration may contribute more to ER, thus exhibiting relatively stronger compensating TRS_{ER}[58]. More productive forests can harbor a greater diversity of plant and microbial species[59]. Communities with a higher number of species possessing diverse thermal niches may better constrain warming-induced respiration increase through species turnover, compared to those with lower biodiversity[60]. As productive tropical and subtropical forests contribute substantially to global CO_2 uptake[2], their strong thermal acclimation capacity, if sustained, is crucial for mitigating future respiratory carbon loss.

Implications of estimated TRS_{ER} on the future terrestrial carbon sink

Our study sheds light on future trends in the global terrestrial ER and carbon sink. First, thermal responses alone could mitigate at least one-fourth of the projected increases in nighttime ER during the growing season across most climates. This mitigation level is comparable to the effects of compensating thermal responses on mitigating leaf respiration increases (e.g., 30~50%)[27,61]. Second, compensating thermal responses, combined with hump-shaped T_S~ER relationships in arid, semi-arid, and Mediterranean climates, and the buffering effects of plant canopy coverage in humid climates, can constrain ER increases to < 10 % of current respiration rates in most climates by 2041-2060. Additionally, when considering the apparent thermal acclimation due to decreased soil water content under continued warming[62], future RE increases could be even lower than our estimate. This projected ER increase rate is much lower than the anticipated GPP increase rate for the same period (11.5 ~ 20%)[63,64], suggesting a low likelihood of ER increase outpacing GPP increase within the projection period. Third, TRS_{ER} may be strengthened by future increase in LAI and primary production in humid tropical, subtropical, and temperate forests[2], due to the nonlinear, threshold-type relationship between TRS_{ER} and LAI[25]. Fourth, despite the overall limited ER increases, large variations in TRS_{ER} and signs of enhancing thermal acclimation were estimated for the cold continental climates (Dfb and Dfc, Figs. 1c and 3a), indicating that ecosystems with little compensating or with enhancing thermal responses may experience large carbon loss with future warming[44]. Lastly, uncertainty remains in both current and future TRS_{ER} for tundra ecosystems, where large quantities of organic carbon are stored in frozen soils[65]. This uncertainty is due to our limited data (n = 3), and the much faster warming rates that may shift some areas from tundra to less extreme climates, such as continental climates, where much weaker compensating TRS_{ER} is observed (Fig. 3a).

Despite using the most extensive and longest CO_2 flux datasets available, our study faces limitations due to the number of flux sites with ≥ 8 years of complete data and their uneven global distribution, including sparse coverage in tropical and Arctic regions. With the rapid increase in flux sites globally[66] and ongoing collection of site-specific soil and vegetation properties[67], future data availability will enable a finer-scale examination of the drivers of TRS_{ER} and better separation of true thermal responses from

apparent ones. This work will be possible by incorporating more site- and species-specific predictor variables, such as soil labile carbon and nutrient contents, and plant traits, while also allowing for global-scale projections of TRS_{ER}. By focusing on nighttime ER only, the T_S~ER relationships are mostly monotonic in climates other than arid, semi-arid, and hot-summer Mediterranean climates (Fig. S6), justifying our method of using the upward and downward shifts in T_S~ER relationships to quantify TRS_{ER} (Figs. 1a-b and S1). However, in hot and dry climates, the T_S~ER relationships may become hump-shaped, and the optimal temperature corresponding to peak ER might also shift with warming[68,69]. How these hump-shaped T_S~ER relationships will change with future warming and their implications for future ER increases merit further investigation.

Overall, our study provides cross-biome converging evidence on the direction, strength, and drivers of *TRS* in ER, soil respiration, and leaf respiration. The widespread prevalence of compensating thermal responses at the ecosystem level, which can mitigate at least one-fourth of future nighttime ER increases across most climates if sustained, may be instrumental in dampening the positive carbon-climate feedback under future warming scenarios. Incorporating these climate-specific TRS_{ER} patterns and their impacts on future ER trajectories (Table S4) into Earth System Models is crucial for enhancing the accuracy of future carbon-climate feedback projections. Concurrently, it is essential to aggressively reduce anthropogenic carbon emissions to prevent large-scale land cover transformation, ecosystem degradation, and the triggering of ecosystem tipping points. These processes could collectively diminish the thermal acclimation potential of natural ecosystems and lead to significant carbon losses from the terrestrial biosphere.

Materials and methods

Quantifying site-specific TRS_{ER}

Following previous studies[27,28], we defined *TRS* of respiration as the response ratio of respiration at a set temperature per degree of temperature increase. The equations to calculate *TRS* are as follows:

$$TRS = \frac{-\ln(Acclim_{T_{set}})}{\Delta T} \quad (1)$$

$$Acclim_{T_{set}} = \frac{R_{control} \text{ at } T_{set}}{R_{treatment} \text{ at } T_{set}} \quad (2)$$

where *TRS* is thermal response strength of a type of respiration (1/°C); T_{set} is a set temperature (°C); $Acclim_{T_{set}}$ is the acclimation ratio at a set temperature (unitless); ΔT is temperature differences between control and treatment conditions (°C); $R_{control}$ at T_{set} and $R_{treatment}$ at T_{set} are the respiration rates measured or estimated at the same set temperature under control and treatment conditions, respectively ($\mu molCO_2\ m^{-2}\ s^{-1}$).

To quantify TRS_{ER} at the ecosystem scale using long-term eddy covariance flux measurements, we modified the above method in three aspects. First, leveraging interannual variations in temperature regimes in natural ecosystems, for a specific site, we treated the average relationship between T_S and ER over all measurement years as the control condition, while the T_S ~ER relationship derived from a specific year's measurements served as the treatment condition. Here, we leveraged interannual temperature variations, as opposed to seasonal temperature variations commonly used for assessing *in-situ* thermal acclimation in leaf respiration[57]. This approach was chosen because thermal acclimation process of soil respiration, a major ER component, typically takes several months, much longer than the few days or weeks required for leaf respiration to acclimate[12,16]. We used most shallow soil temperature (depth < 0.1 m) to represent temperature regime, as our model testing indicates that ER is more correlated with T_S than with air temperature, with R^2 values being, on average, 0.03 higher for T_S across all sites. Second, we focused on the average TRS_{ER} during the growing season (defined later), since ER during the growing seasons often accounts for the majority of annual ER[70]. Specifically, for each year, we calculated acclimation ratios at multiple set temperatures within the growing-season temperature range and used their weighted average (i.e., $\overline{Acclim_{T_{set}}}$), with $R_{control}$ at T_{set} serving as the weights, to represent this year' acclimation

ratio. We also calculated the mean T_S of the growing season ($\overline{T_S}$) for each year. Finally, we fit a linear regression between $-\ln(\overline{Acclim_{T_{set}}})$ and $\overline{T_S}$, using the regression slope to measure TRS_{ER}. The Fig. S1 illustrates the three steps using the AmeriFlux grassland site US-IB2 as an example. Below, we describe in detail the selection of study sites and data, the development of T_S~ER model, and the calculation and the assessment of TRS_{ER}.

Study site selection and data pre-processing. To ensure our method can quantify TRS_{ER} for a variety of terrestrial ecosystems and that the TRS_{ER} estimates are minimally affected by gaps and errors in eddy covariance flux measurements, we defined specific criteria for selecting study sites, years, and measured nighttime ER data. We first selected AmeriFlux, ICOS[71], FLUXNET sites with $\geq$ 8 years of CO_2 flux, air and soil temperature data, excluding all sites described as croplands, or highly managed grasslands, or at early succession stage. To ensure accurate estimate of TRS_{ER}, we set the minimum data duration to 8 years, as it is recommended to have > 5 data points to obtain a reliable estimation of the linear regression slope[72] (Fig. S1c). For each site, we removed years with single CO_2 flux measurement gaps longer than one month during the growing season, as long gaps may result in biased T_S~ER relationships. After applying these criteria, we selected 93 sites with $\geq$ 8 years of complete data for further analysis (Table S1).

For the selected sites, we only used hourly or half-hourly CO_2 fluxes measured during the night after the correction of storage fluxes. This is because eddy covariance towers measure NEP which is the difference between GPP and ER during the daytime, and at night NEP is equal to ER assuming negligible lateral fluxes. Although daytime ER can be estimated by partitioning GPP and ER, this involves extra assumptions such as the extrapolation of short-term T_S~ER relationship[73], potentially adding artificial effects to the true T_S~ER relationship. Emerging partitioning methods using stable C isotopes and solar-induced chlorophyll fluorescence suggest extrapolating nighttime T_S~ER relationships could overestimate daytime ER due to light inhibition of daytime ER[74–76]. As stable stratification and low turbulence mixing at night may induce large errors in flux measurements, we selected Ustar (friction velocity) filtered nighttime ER data at FLUXNET sites, using a variable Ustar threshold for each year. To ensure comparable processing of data, we used the R package *REddyProc*[77], developed following FLUXNET protocols, to select nighttime ER data with

Ustar values greater than yearly Ustar thresholds at AmeriFlux sites. Therefore, this study only used directly measured, high-quality nighttime ER data.

Additionally, T_S measurements were incomplete for certain sites (17 sites). In these cases, we implemented a random forest model to predict missing T_S based on air temperature and the day of the year. The R^2 of these T_S models exceeded 0.9 for testing datasets.

The T_S~ER relationships. Globally, ER is primarily regulated by temperature and water availability[78]. Here, we used T_S and soil water content (W_S) of the topsoil layer to represent the temperature and water availability at each site. Since thermal responses of respiration generally refers to the direct responses of organisms to temperature changes that manifest as changes in temperature-respiration relationships[14,17], and temperature can indirectly affect respiration via altering W_S (e.g., warming can reduce soil respiration by decreasing W_S)[22], we incorporated both T_S and W_S into the ER model to capture the direct effects of T_S on ER. We used an exponential-quadratic relationship to quantify the effects of T_S, as this relationship can represent both monotonic and hump-shaped T_s~ER patterns observed across different ecosystems[9]. This model performed slightly better than the simple exponential (Q_{10} method), quadratic[68], and modified Arrhenius models[73]. Following previous studies[9,79], we used the Michaelis-Menten equation to quantify the effects of W_S on ER. The respiration model is given by:

$$ER = \gamma e^{\alpha T_S + \beta {T_S}^2} \frac{W_S}{H_S + W_S} \quad (3)$$

where γ, α, and β are parameters in the exponential-quadratic relationship between T_S and ER, and H_S is half saturation constant (%). In this model, ER varies with both T_s and W_S. To obtain T_s~ER relationships, we fixed W_S at a site-specific constant value (i.e., the mean W_S across all selected years). For each site, we obtained an individual T_s~ER curve for each year (treatment curves) and an overall T_s~ER curve for all years (the control curve) (Fig. S1a).

It is important to note that 39 of our sites have too few W_S data (i.e., more than one-month missing W_S data in the growing season) to be included in the respiration model (Table S1). For these sites, we removed the W_S term (i.e., $\frac{W_S}{H_S+W_S}$) from Eq. (3) when obtaining T_s~ER curves. To understand when

removing W_S term affects TRS_{ER} estimates, we obtained another set of T_s ~ER curves for the 54 sites with enough soil water data using the respiration mode without the W_S term (i.e., $ER = \gamma e^{\alpha T_S + \beta T_S^2}$), and compared TRS_{ER} values estimated from the two different sets of T_s~ER curves. The comparison, shown in Fig. S7, indicates that including the W_S term in the respiration model primarily affects the TRS_{ER} estimates at five semi-arid sites (US-SRG, US-SRM, US-Whs, US-Wkg, and ZA-Kru), two evergreen broadleaf forest sites (AU-Tum and FR-Pue), and one site (CZ-BK1) at humid continental climate. Because all arid and semi-arid sites, as well as evergreen broadleaf forest sites, have sufficient W_S data (Table S1), and most sites in the humid continental climate show similar TRS_{ER} values regardless of controlling for W_S (Fig. S7b), not including W_S in the respiration model at other sites likely has minimal effects on the TRS_{ER} calculation.

The model to calculate TRS_{ER}. For a given site, we first identified the T_S range for the growing season. We defined the growing season as the period when daily NEP is above 0.8 g C m^{-2} or above 20% of maximum daily NEP within a year for five consecutive days[70]. We defined the growing-season T_S as the range between the 2.5th and 97.5th percentiles of the nighttime T_S measured during the growing season. We then divided this temperature range into intervals of 0.1 ℃, using interval endpoints as set temperatures.

For each year (i), we used the T_s~ER curve for this year as the treatment, and the average T_s~ER curve across all years as the control. We calculated the acclimation ratio at each set temperature using Eq. (2) and took a weighted average of these acclimation ratios for each year ($\overline{Acclim_{T_{set}}}_i$) using control respiration at each set temperature as the weights (Fig. S1b). We also calculated the average growing-season T_S for each year ($\overline{T_S}_i$). By repeating this step, we obtained $\overline{Acclim_{T_{set}}}$ and $\overline{T_S}$ for all years. Lastly, we built a linear regression model between $-\ln(\overline{Acclim_{T_{set}}})$ and $\overline{T_S}$ to calculate TRS_{ER} (i.e., the regression slope of $\overline{T_S}$) (Fig. S1c). The regression model is given as:

$$-\ln\left(\overline{Acclim_{T_{set}}}\right) = \beta_0 + \beta_1 \overline{T_S} + \epsilon \quad (4)$$

where β_0 is the intercept, β_1 is the regression slope (i.e., TRS_{ER}), and ϵ is the error term. We used the significance level (i.e., p-value) of β_1 to indicate if TRS_{ER} was statistically significant. We categorized a site as exhibiting a

694 significant compensating thermal response if the *p*-value was < 0.1 and
695 TRS_{ER} was negative (i.e., lower ER rates at a set temperature in a warmer
696 year). If the *p*-value was < 0.1 and TRS_{ER} was positive, we categorized the
697 site as having a significant enhancing thermal response. Given that
698 approximately 70 % of the study sites have fewer than 15 years of complete
699 data, a significance level of 0.1 was used to report if a site had statistically a
700 significant thermal response; however, we also reported sites with
701 estimated TRS_{ER} at a 0.05 significance level (Table S1).

702 **The assessment of estimated TRS_{ER}.** To assess our method of quantifying
703 *TRS* at the ecosystem level using eddy covariance flux data, we compared
704 TRS_{ER} estimated by this method with *TRS* of leaf, root, and soil respiration
705 estimated from *in-situ* warming experiments or field measurements in the
706 literature. We did not compare our results with lab experiments due to the
707 dramatic differences between lab and field environments, such as the over
708 10°C warming magnitudes in many lab experiments[28]. Specifically, we
709 searched the Web of Science database using the keywords “respiration”,
710 “acclimation”, and “warming”, and found 21 studies that detected thermal
711 acclimation in at least one type of respiration (leaf, root, or soil) and
712 provided enough data to calculate *TRS* using Eqs. (1-2). Most of these
713 studies measured respiration at a set temperature of 20 °C. For studies that
714 did not specify a set temperature, we used the mean of measurement
715 temperatures as the set temperature to calculate *TRS*. The calculated *TRS*
716 values from these studies are listed in Table S2.

717 Among the 21 studies, one was conducted in the region where we found a
718 matching eddy covariance site with the same climate, vegetation class, and
719 similar latitude. An AmeriFlux grassland site in the Great Plains (US-Kon,
720 Latitude: 39.08□, Longitude: -96.56□) matches the soil warming experiment
721 by Luo et al., 2001[26] (Latitude: 34.98□, Longitude: -97.52□). For the
722 matching sites, we compared TRS_{ER} estimated by our method with *TRS*
723 derived from this experiment.

724 Analyzing the factors affecting TRS_{ER}

725 **Predictor variables and data sources.** Previous studies have explored
726 factors affecting *TRS* of leaf and soil respiration separately. *TRS* of leaf
727 respiration is influenced by elevation, mean temperature, temperature
728 variation, leaf forms (needleleaf vs. broadleaf), and leaf age[16,28,35]. *TRS* of
729 soil respiration is also affected by soil properties such as soil carbon content
730 and carbon-to-

nitrogen ratios, in addition to climate factors[12,31,44,80]. It is likely that ecosystem-scale TRS_{ER} is also affected by geographic, climatic, vegetation and soil variables, albeit with varying degrees of importance. Moreover, primary productivity, such as GPP, may shape TRS_{ER}. We defined 11 variables to characterize these factors (Table S3).

We used elevation (ELEV, m) to represent geographic effects, including extreme environment at high elevations like limited resources and low productivities. We used mean annual precipitation (MAP, mm), mean annual air temperature (MAT, °C), air temperature seasonality (SST), daily air temperature range (DRT, °C), and interannual air temperature variation (IAT) to quantify precipitation and temperature regimes. We used soil organic carbon stock of the top 0.3 m layer (SOC, t ha^{-1}) where most soil respiration occurs[81] to describe soil properties. We used four variables to characterize vegetation properties: mean annual normalized difference vegetation index (NDVI), mean annual enhanced vegetation index (EVI), mean annual leaf area index (LAI), and mean annual gross primary productivity (GPP, kg C m^{-2} yr^{-1}). Geographic and climatic variables were calculated using field-measured data. The soil variable SOC was estimated by combining field measurements from 25 sites with data from global soil organic carbon maps at a 1 km^2 resolution (GSOCmap V1.5)[82]. The measured SOC from the 25 sites was significantly correlated with the SOC values extracted from the GSOCmap at the same locations ($p < 0.05$), supporting the use of SOC from global maps for sites without direct measurements. Vegetation properties including GPP were derived from NASA's moderate resolution imaging spectroradiometer (MODIS) product (2002-2020, 16-day interval). We used remotely sensed GPP because some sites do not have GPP partitioned from NEP.

Predictor variable correlation and selection. To assess collinearity among predictor variables, we calculated Pearson correlation coefficients (r) between pair of variables (Fig. S2). To avoid interpretation issues from highly correlated predictors in regression models, we selected four representative variables with low correlation (r < 0.4) from the 11 variables (Table S3). Specifically, as the four variables describing temperature regime are all significantly correlated, we used MAT to represent temperature regime. Similarly, as all vegetation variables are highly correlated, we chose LAI to represent vegetation properties. Moreover, as LAI is strongly correlated to precipitation (MAP), we removed MAP. The

variance inflation factors of the four selected variables (i.e., ELEV, MAT, SOC, and LAI) are all lower than 1.3, suggesting low multicollinearity among them.

Random forest model for driver analysis. We used a random forest model to analyze how TRS_{ER} varied with each representative variable, as this model can capture complex nonlinear relationships[83]. To prevent overfitting, we applied five-fold cross-validation to determine the number of predictors sampled for splitting at each node (set to 1) and the minimum size of terminal nodes (set to 24). The model was built with 500 trees to calculate relative importance and partial dependence (i.e., marginal effect) of each selected predictor variable. Variable's relative importance was estimated by permutation-based MSE (i.e., mean squared error) reduction method. Model uncertainty was gauged using bootstrapping to build 200 random forest models, estimating 90 % confidence intervals for each variable's relative importance and partial dependence.

Projecting the effects of thermal responses on mediating future ER

To estimate how much future nighttime ER might be reduced or increased due to compensating or enhancing thermal response at each site, we applied site-specific TRS_{ER} and projected future air temperature change to established respiration models in three steps, under the assumption of no land cover changes by 2041-2060. First, we obtained predicted monthly air temperature changes from the current period (2001-2020), when most eddy covariance data were collected, to the future period (2041-2060). Global monthly minimum air temperature with a 30-second spatial resolution were downloaded from worldclim.org for the current period (2001-2020) and for the future period (2041-2060) under the medium pathway of future greenhouse gas emissions (SSP245) using the ensemble average of 12 Earth System Models (i.e., ACCESS-CM2, BCC-CSM2-MR, CMCC-ESM2, EC-Earth3-Veg, FIO-ESM-2-0, GISS-E2-1-G, HadGEM3-GC31-LL, INM-CM5-0, IPSL-CM6A-LR, MIROC6, MPI-ESM1-2-HR, and UKESM1-0-LL). We chose minimum temperature instead of mean temperature because our study centers on nighttime ER, and asymmetric warming between day and night may occur at some sites[84]. To derive monthly air temperature change from 2001-2020 to 2041-2060, we subtracted the monthly air temperature for 2001-2020 from those for 2041-2060. We extracted monthly air temperature changes at the grids where each study site is located. Additionally, we converted air temperature change to topsoil temperature change by

multiplying the monthly air temperature change by the site-specific regression slope of topsoil temperature on air temperature, as topsoil temperature was used to predict ER (Eq. (3)).

Next, we determined the current and future topsoil temperature and water regimes for each site. We obtained the current annual topsoil temperature regime at the hourly timescale by averaging nighttime topsoil temperature measured on the same hour and the same day of year across all years. Similarly, we got the current annual soil water content regime. To obtain the future topsoil temperature regime, we added the predicted monthly topsoil temperature changes to the corresponding month of the current temperature regime. For simplicity, we assumed the future soil water content regime to be the same as the current regime. While this assumption may be unrealistic for some sites (e.g., semi-arid), it may not compromise our primary focus on the effects of thermal responses (i.e., direct responses of biological communities to temperature change) on future ER. This assumption may lead to slight overestimation of future ER increase, as warming generally reduces soil water content and ER[78].

Lastly, we calculated four annual growing-season nighttime ER metrics for each site. The first is the current annual growing-season nighttime ER, calculated based on current topsoil temperature and water content regimes using the established respiration model when obtaining the average T_s~ER relationships (Eq. (3)). The second is the future annual growing-season nighttime ER without thermal response (the “no thermal response” scenario), calculated using the same respiration model but based on the future topsoil temperature and water content. The third is the future annual growing-season nighttime ER with estimated TRS_{ER} for all sites (the “all thermal responses” scenario). It was calculated by multiplying the future annual growing-season nighttime ER (the second metric) by $e^{TRS_{ER} \cdot \Delta T_s}$ to account for the effects of TRS_{ER} and the change in growing-season topsoil temperature (ΔT_s). If this metric is lower than the first metric (i.e., overcompensation, which has been observed in experiments)[85], we assumed it to be equal to the first metric to obtain a conservative estimate of the effects of thermal acclimation. The last is the future annual growing-season nighttime ER with thermal responses, but only at sites with significant TRS_{ER} (the “significant thermal responses” scenario), accounting for the uncertainty in estimating TRS_{ER}. We compared the four metrics and the changes in future ER relative to current ER across every climate class to understand how compensating or enhancing thermal responses affect future

ER differently across climate classes (Figs. 4 and S4). It is worth noting that ΔT_s at most sites are < 2 °C and lower than the interannual difference in mean growing-season T_S observed in the years used to estimate TRS_{ER} (Fig. S8). This suggests a low risk of extrapolation and justifies the use of the TRS_{ER} derived from the past decades to project their effects in 2041-2060.

Acknowledgements

We sincerely thank Dr. Mark A. Bradford for his insightful and constructive feedback on the manuscript. We acknowledge the principal investigators who provided data for our study sites but are not listed as authors. Support for this work was provided by the U.S. National Science Foundation (NSF) (#2047687 and #2330792), the Yale School of the Environment, and the Yale Center for Natural Carbon Capture. D.A.R was supported by Department of Energy Ameriflux Management Project Core Site Funding to ChEAS (cluster #7544821) and U.S. NSF (#2313772). L.Š. received funding from the Ministry of Education, Youth and Sports of CR within the CzeCOS program (LM2023048) and AdAgriF project (CZ.02.01.01/00/22_008/0004635). A.K. was funded by Niedersächsisches Vorab (ZN 3679), Ministry of Lower-Saxony for Science and Culture, and Volkswagen Foundation. M.U. was funded by Arctic Challenge for Sustainability II (ArCS II; JPMXD1420318865). E.P.S. received fundings through projects PID2020-117825GB-C21 and PID2020-117825GB-C22. G.S. was funded by U.S. NSF (DEB#1910811). M.P. was funded by the Swedish Research Council and contributing research institutes.

Code availability

Code used in the analysis of this paper is available online in the repository: https://github.com/jnawang/thermal_acclimation_in_ecosystem_respiration.

Data availability

This work used publicly available AmeriFlux, ICOS, and FLUXNET eddy covariance data, which were downloaded at https://ameriflux.lbl.gov, https://www.icos-cp.eu/data-products/2G60-ZHAK, and https://fluxnet.org/data/fluxnet2015-dataset/.

Supplementary information:

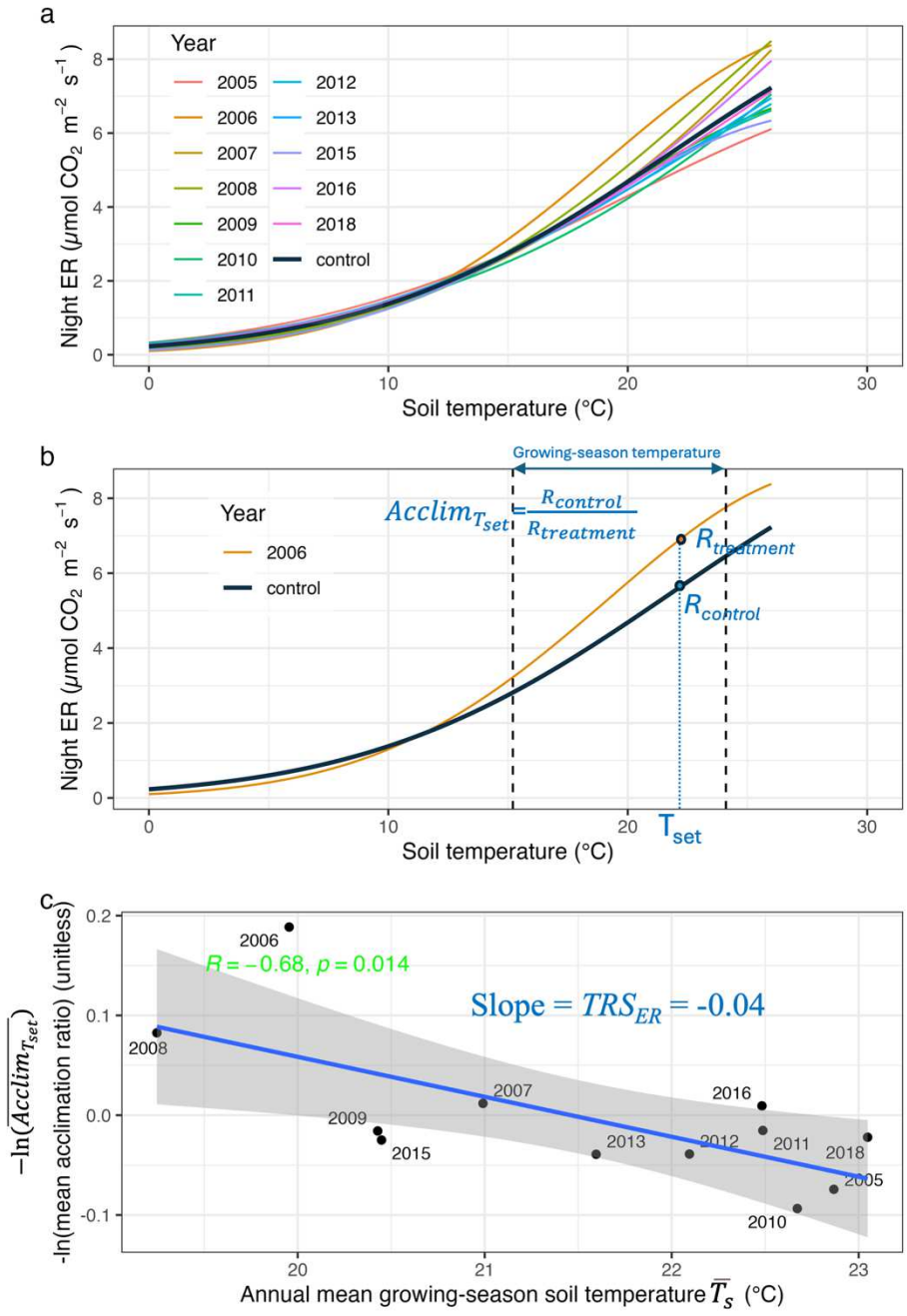

Figure S1. Illustration of the three steps for estimating thermal response strength of ecosystem respiration (TRS_{ER}) using the site US-IB2 as an example: (a) fit a curve between topsoil temperature (T_s) and nighttime ecosystem respiration (ER) (i.e., T_s~ER curve) for each year (i.e., treatment conditions) and all the years (i.e., the control condition), (b) calculate average acclimation ratios over the growing-season temperature range for each year ($\overline{Acclim_{T_{set}}}$), and (c) conduct a linear regression between the

annual mean growing-season topsoil temperature ($\overline{T_s}$) and $-\ln(\overline{Acclim_{T_{set}}})$, with the regression slope representing TRS_{ER}.

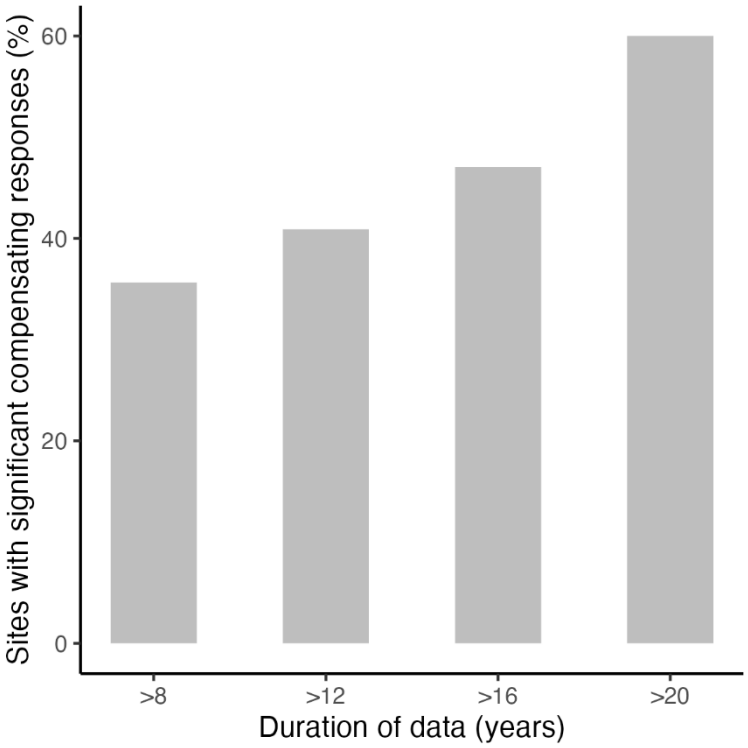

Figure S2. The fraction of sites with significant compensating thermal responses increases with the duration of CO_2 flux data.

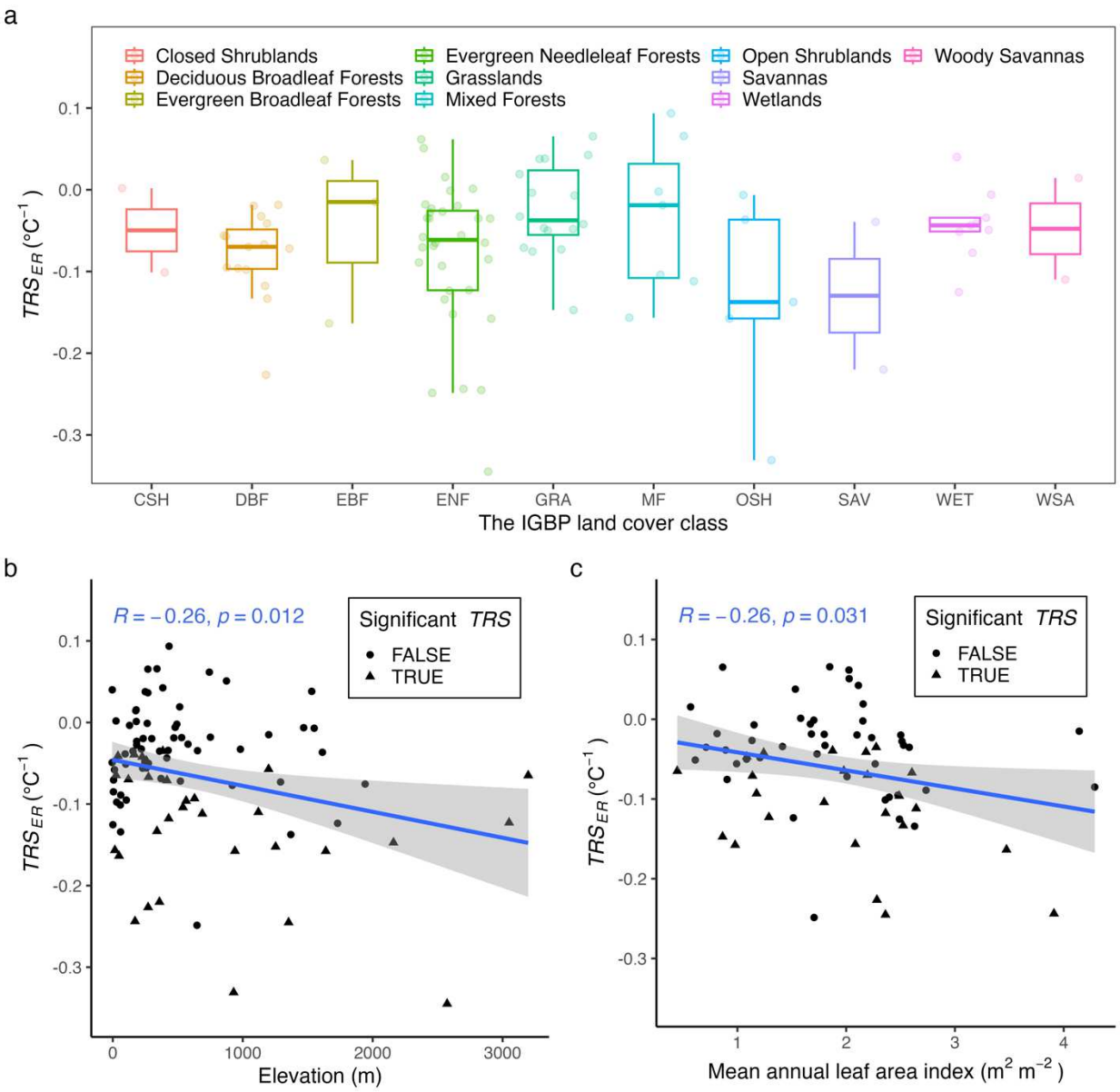

Figure S3. Variations in thermal response strength of ecosystem respiration (TRS_{ER}) with IGBP land cover class, elevation, and mean annual leaf area index, revealed by univariate analysis. (a) No significant difference in TRS_{ER} is observed among the various IGBP land cover classes ($n = 93$, $p = 0.19$ by analysis of variance). (b) The magnitude of compensating TRS_{ER} increases with elevation (more negative) across all study sites ($n = 93$). (c) For sites in humid climates (i.e., humid tropical, subtropical, and continental climates; $n = 69$), the magnitude of compensating TRS_{ER} increases with mean annual leaf area index (more negative). The trends shown in (b) and (c) from the linear univariate analysis are consistent with the partial dependence plots from the random forest model (Fig. 3c-d),

except that the random forest model can capture highly nonlinear relationships.

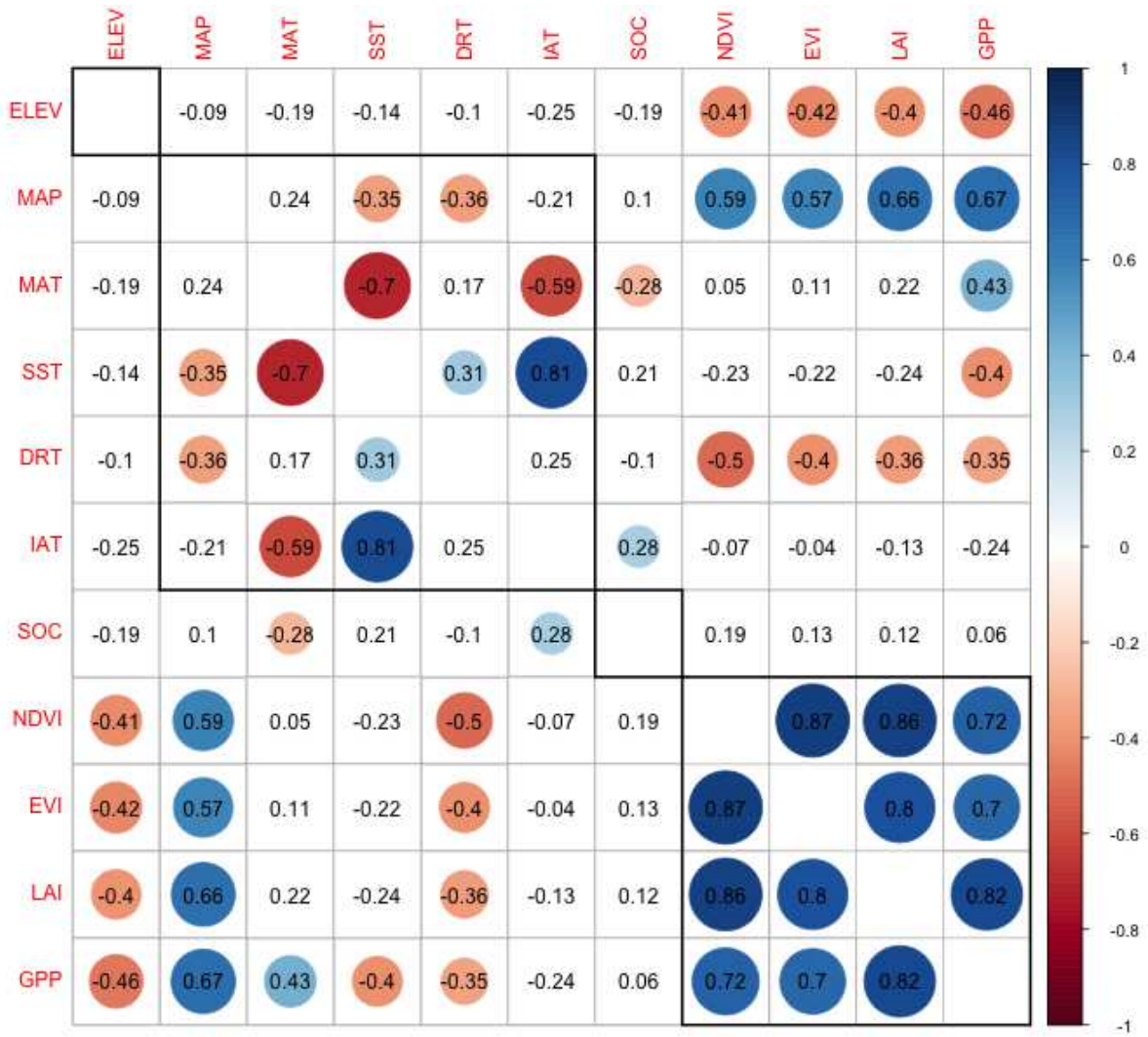

Figure S4. Pearson correlation matrix between any two variables potentially affecting TRS_{ER} (See Table S3 for the definitions of these variables). The numbers represent the correlation coefficients. Circles indicate correlations above the 0.01 significance level, with red circles representing negative correlations and blue circles indicating positive correlations. Variables within a bold square belong to one category.

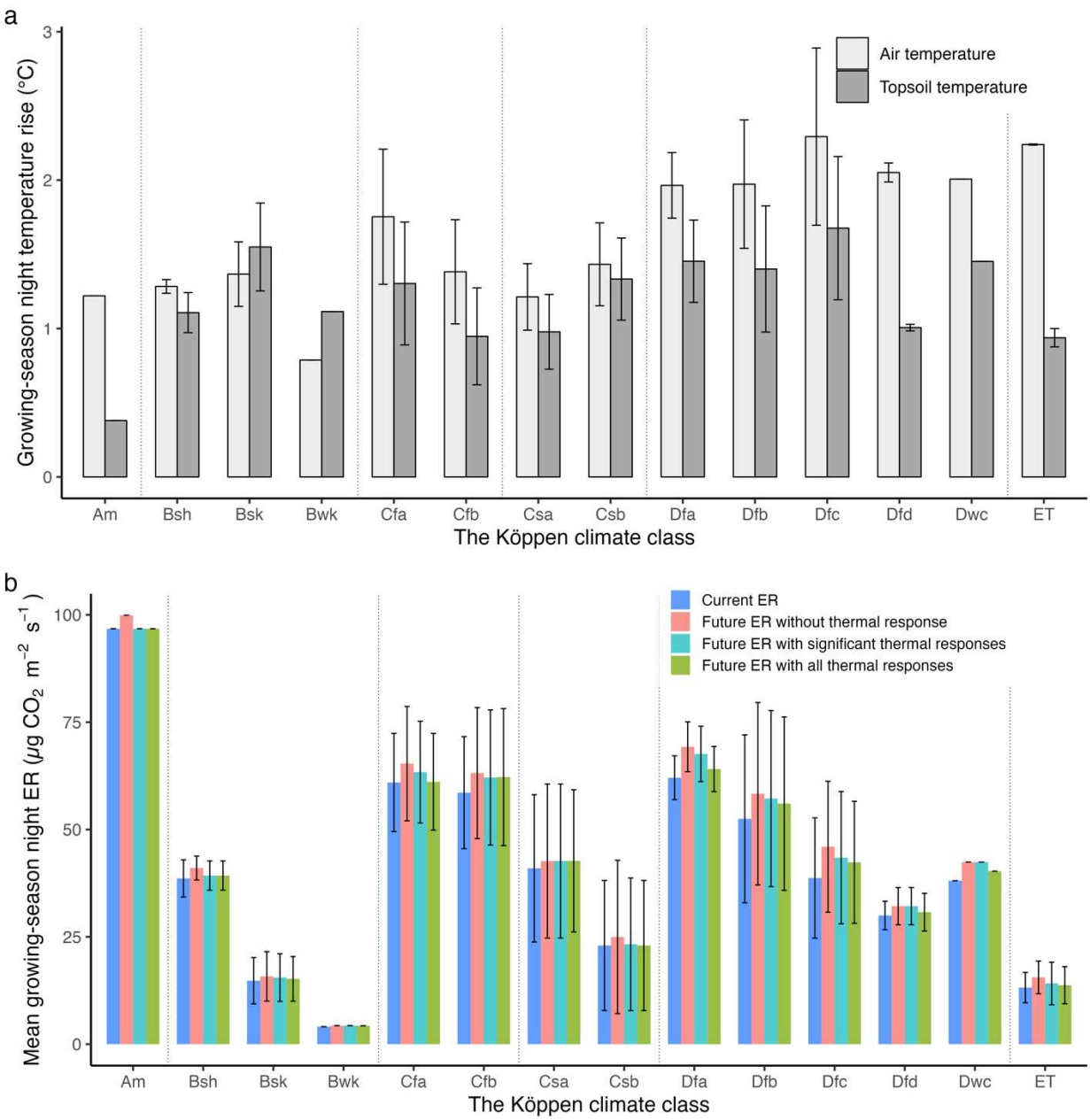

Figure S5. Growing-season nighttime air and topsoil (depth < 0.1 m) temperature rise from 2000-2020 to 2041-2060 at the study sites grouped by the Köppen climate classes (a) and the responses of future nighttime ecosystem respiration (ER) with and without considering thermal responses (b) under the medium warming scenario (SSP245). Error bars denote standard deviation of temperature and ER for sites in the same climate class. In (b), future ER with all thermal responses was calculated using estimated TRS_{ER} for all sites, while future ER with significant thermal

responses was calculated assuming no thermal response for sites with non-significant TRS_{ER} ($p > 0.1$).

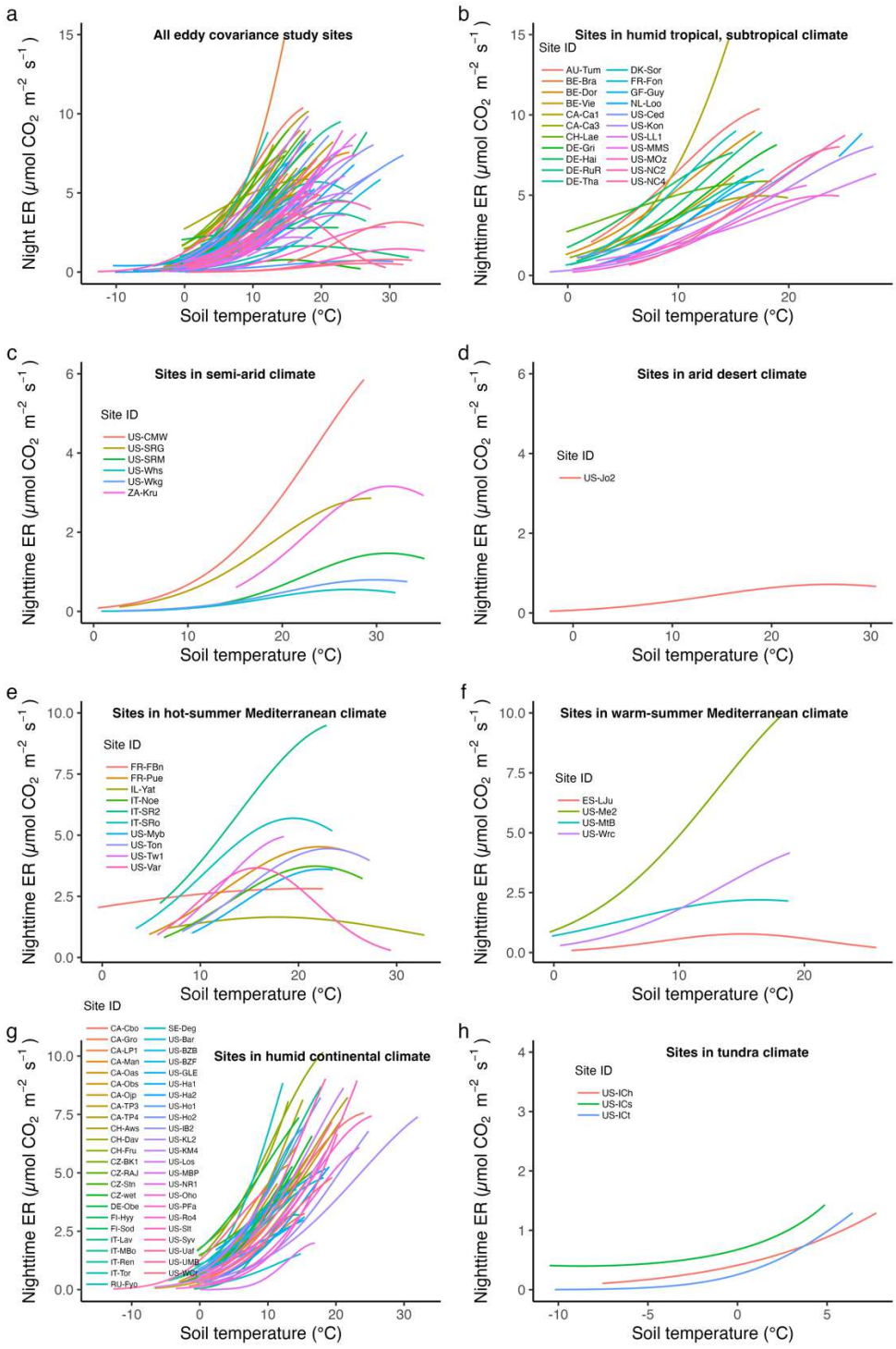

Figure S6. Relationships between topsoil temperature and nighttime ecosystem respiration (ER) for all the study sites (a), for sites in humid tropical, subtropical climate (b), in semi-arid climate (c), in arid desert climate (d), in hot-summer (e) and warm-summer (f) Mediterranean climate, in humid continental climate (g), and in tundra climate (h). Note: two sites

in (e), US-Tw1 and US-Myb, which do not display clear hump-shaped temperature~ER relationships are wetlands.

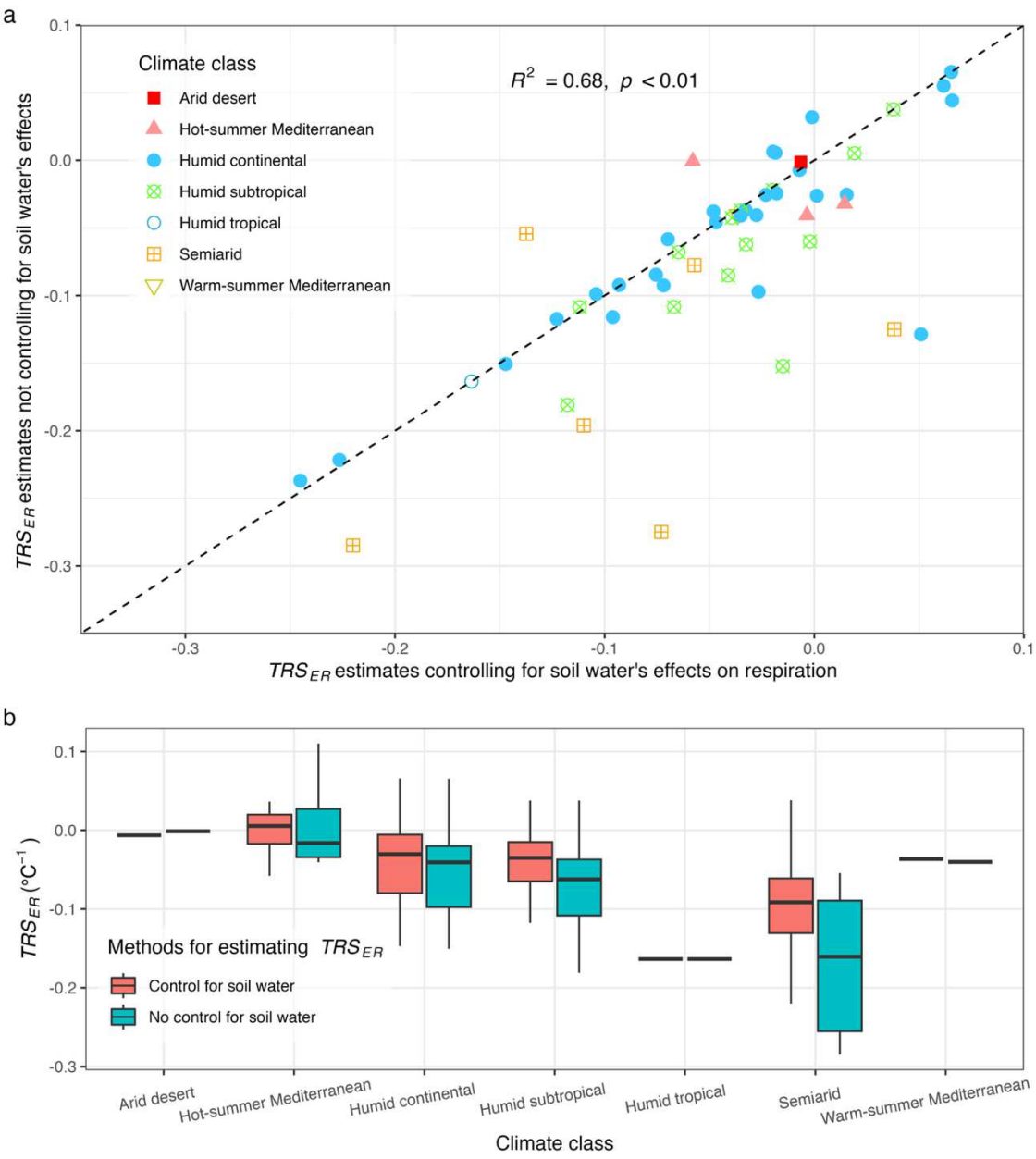

Figure S7. Comparison of TRS_{ER} estimates using respiration models with and without controlling for the effects of soil water content. This figure compares TRS_{ER} estimates derived from respiration models that either control for the direct effects of soil water content (Eq. (3)) or exclude these effects (i.e., removing the soil water term from Eq. (3)) for 54 flux sites with sufficient soil water measurements. (a) Overall comparison of TRS_{ER} estimates from the two methods at the 54 sites. The black dashed line represents the 1:1 line. (b) Comparison of TRS_{ER} estimates from the two methods by climate class. In semi-arid sites, controlling for soil water's effects generally reduced the magnitude of estimated TRS_{ER} (less negative)

except for one site (US-Whs). For sites in other climates (e.g., arid, Mediterranean, and humid), the two methods generally provided similar estimates.

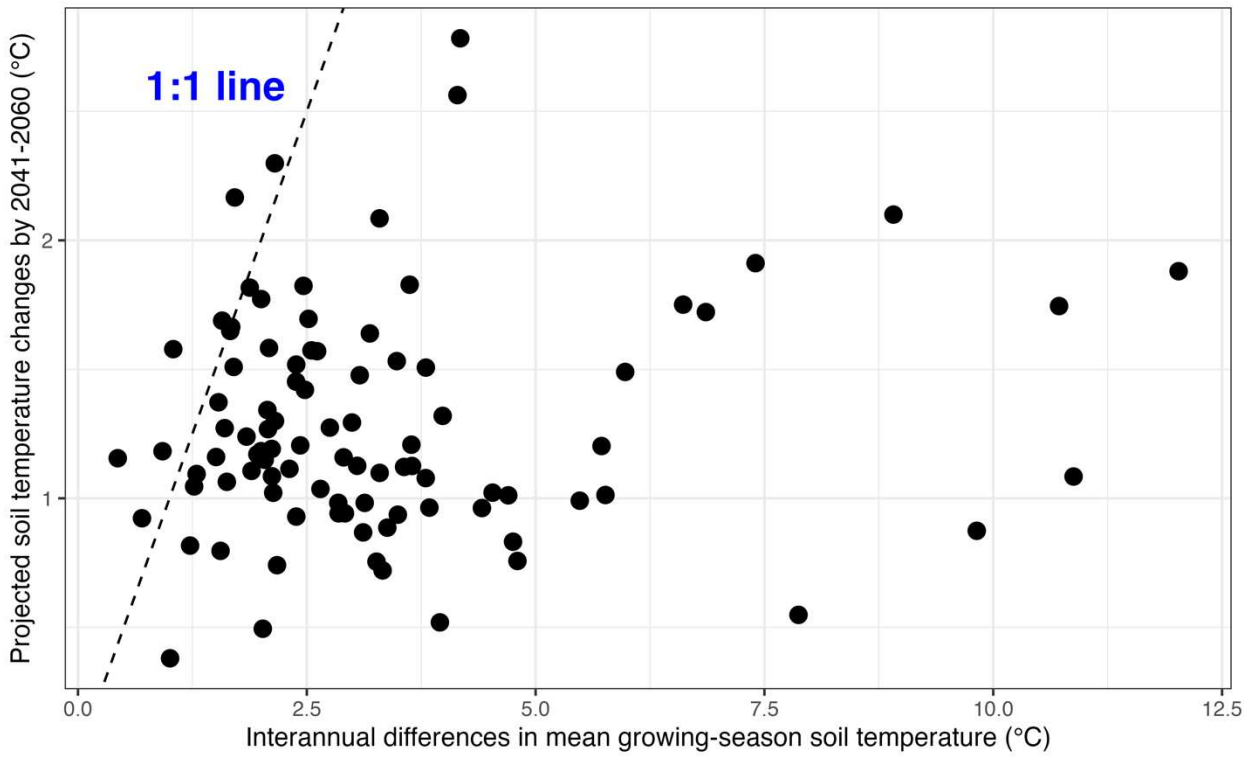

Figure S8. Comparison of interannual differences in mean growing-season topsoil temperature and projected topsoil temperature changes (2041-2060 under medium greenhouse gas emissions scenario: SSP245) for each study site. This figure shows that, for most sites (86 out of 93), interannual differences in mean growing-season topsoil temperature exceed projected topsoil temperature changes (below the 1:1 line). This suggests that using TRS_{ER} derived from long-term observations over the past one to three decades to project the effects of thermal acclimation on future ecosystem respiration in 2041-2060 is unlikely to suffer from extrapolation errors or biased estimates for most sites.

Table S1. Climate, vegetation, and ecosystem characteristics of the 93 eddy covariance flux sites, along with the estimated thermal response strength of ecosystem respiration (TRS_{ER}).

Köppen climate class	Study sites	Vegetation class	Soil water used or not	Number of years	Mean annual air temperature (℃)	Mean annual precipitation (mm)	Mean annual net ecosystem productivity (g C m^{-2})	TRS_{ER} ($℃^{-1}$)
Am	GF-Guy	EBF	YES	13	25.66	3041	242.09	-0.164**
Bsh	US-CMW	DBF	YES	17	17.01	288	369.04	-0.057**
Bsh	ZA-Kru	SAV	YES	10	21.86	547	44.58	-0.220**
Bsk	US-Wkg	GRA	YES	17	17.47	407	34.95	0.038
Bsk	US-SRM	WSA	YES	17	19.19	380	2.05	-0.110**
Bsk	US-Whs	OSH	YES	15	17.12	320	-15.04	-0.137
Bsk	US-SRG	GRA	YES	16	18.94	420	41.94	-0.073
Bwk	US-Jo2	OSH	YES	10	17.64	282.3	174.96	-0.006
Cfa	US-MMS	DBF	YES	23	12.46	1032	357.65	-0.067**
Cfa	US-Kon	GRA	NO	11	13.15	867	163.00	-0.071**
Cfa	US-MOz	DBF	YES	14	13.53	986	364.68	-0.033
Cfa	US-NC2	ENF	NO	11	15.99	1320	531.90	-0.085
Cfa	US-LL1	SAV	YES	12	19.42	1310	203.97	-0.039*
Cfa	US-NC4	WET	NO	10	17.04	1311	-38.72	-0.125
Cfa	US-Ced	CSH	NO	9	12.03	1138	80.63	-0.101
Cfb	CA-Ca3	ENF	NO	13	12.11	1676	401.96	-0.244**
Cfb	CA-Ca1	ENF	YES	12	8.07	1369	373.76	-0.020
Cfb	AU-Tum	EBF	YES	10	9.63	1159	592.43	-0.015
Cfb	BE-Bra	MF	NO	14	11.07	750	127.31	-0.157*
Cfb	BE-Vie	MF	YES	24	8.62	1062	473.58	-0.002
Cfb	CH-Lae	MF	YES	13	8.44	1100	281.36	-0.112**
Cfb	DE-Gri	GRA	NO	15	8.65	901	82.98	0.042
Cfb	DE-Hai	DBF	YES	18	8.54	720	523.22	-0.118**
Cfb	DE-Tha	ENF	YES	24	9.24	843	469.55	-0.035**
Cfb	DK-Sor	DBF	YES	21	8.72	660	214.94	-0.041**
Cfb	NL-Loo	ENF	YES	14	10.14	786	473.04	-0.065**
Cfb	BE-Dor	GRA	YES	11	10.06	581.8	73.94	0.038
Cfb	DE-RuR	GRA	YES	10	8.43	1033	118.02	0.019
Cfb	FR-Fon	DBF	NO	16	11.73	720	603.69	-0.095

Csa	US-Var	GRA	YES	19	16.07	559	2.38	-0.004
Csa	US-Ton	WSA	YES	16	16.50	559	87.79	0.014
Csa	US-Myb	WET	NO	10	15.63	338	412.36	0.040
Csa	US-Tw1	WET	NO	11	14.99	421	269.50	-0.049
Csa	FR-Pue	EBF	YES	13	14.13	883	347.80	0.036
Csa	IT-Noe	CSH	NO	8	16.40	588	192.51	0.002
Csa	IT-SRo	ENF	NO	10	15.22	920	383.80	-0.071
Csa	FR-FBn	MF	NO	11	14.02	700	558.68	0.094
Csa	IL-Yat	ENF	NO	15	18.43	285	135.99	-0.035
Csa	IT-SR2	ENF	YES	8	15.71	920	225.85	-0.058
Csb	US-Me2	ENF	NO	10	7.99	523	352.60	-0.152*
Csb	US-MtB	ENF	NO	9	9.89	790	495.35	-0.345*
Csb	US-Wrc	ENF	NO	9	9.25	2452	273.83	-0.069
Csb	ES-LJu	OSH	YES	12	11.86	400	3.29	-0.037
Dfa	US-IB2	GRA	NO	12	9.22	930.25	215.19	-0.042**
Dfa	US-KL2	GRA	YES	13	9.32	1027	263.12	-0.047**
Dfa	US-Ro4	GRA	NO	10	7.47	879	281.71	-0.050
Dfa	US-KM4	GRA	YES	12	9.20	1027	6.01	-0.048
Dfa	US-Oho	DBF	NO	10	10.50	849	783.73	-0.056
Dfa	US-Slt	DBF	NO	10	12.34	1138	-8.65	-0.098
Dfb	CA-Cbo	DBF	YES	13	7.40	876.34	317.77	-0.070**
Dfb	US-Ha1	DBF	NO	17	8.33	1071	249.88	-0.133*
Dfb	US-Ha2	ENF	NO	14	8.38	1071	451.45	-0.035
Dfb	US-Los	WET	NO	14	5.14	828	97.09	-0.006
Dfb	US-Ho1	ENF	NO	18	6.38	1070	301.47	-0.134
Dfb	US-Ho2	ENF	NO	18	7.30	1064	310.77	-0.089
Dfb	US-WCr	DBF	YES	14	5.29	787	264.61	-0.072
Dfb	US-UMB	DBF	YES	11	7.16	803	205.28	-0.020
Dfb	US-PFa	MF	NO	13	5.43	823	-7.98	-0.019
Dfb	US-Syv	MF	YES	10	4.56	826	150.44	-0.104*
Dfb	US-Bar	DBF	YES	12	7.41	1245.77	215.12	-0.227**
Dfb	CA-TP4	ENF	YES	14	9.31	1036	167.49	-0.028
Dfb	CA-TP3	ENF	YES	10	9.06	1036	503.71	-0.023
Dfb	CA-LP1	ENF	YES	10	2.89	570	175.88	-0.018
Dfb	CA-Gro	MF	YES	8	3.75	831	118.19	0.066
Dfb	US-MBP	WET	NO	12	4.11	780	221.42	-0.044
Dfb	CZ-BK1	ENF	YES	15	6.90	1316	831.15	0.051
Dfb	CZ-wet	WET	NO	11	8.77	604	-45.16	-0.034
Dfb	IT-Lav	ENF	YES	14	7.30	1291	1965.12	-0.245**
Dfb	IT-MBo	GRA	YES	15	5.43	1214	31.02	-0.007
Dfb	RU-Fyo	ENF	YES	19	5.41	711	-93.58	-0.001
Dfb	CH-Fru	GRA	YES	13	7.89	1651	205.84	-0.033
Dfb	CZ-RAJ	ENF	NO	8	8.15	681	538.02	-0.249
Dfb	CZ-Stn	DBF	YES	11	9.06	685	247.12	-0.096**
Dfb	DE-Obe	ENF	YES	10	6.75	996	259.49	0.062
Dfc	US-GLE	ENF	NO	13	0.33	1200	42.17	-0.065*

Dfc	US-NR1	ENF	YES	19	2.35	800	196.56	-0.123**
Dfc	CA-Oas	DBF	YES	14	1.92	428.53	129.57	-0.019
Dfc	CA-Man	ENF	NO	12	-1.18	520	-0.59	-0.056
Dfc	CA-Obs	ENF	YES	11	1.21	405.6	54.98	-0.093**
Dfc	CA-Ojp	ENF	YES	11	1.44	430.5	38.12	-0.027
Dfc	FI-Hyy	ENF	YES	24	4.56	709	231.37	0.001
Dfc	FI-Sod	ENF	YES	10	0.81	500	-94.62	0.015
Dfc	IT-Ren	ENF	NO	18	4.86	809.3	667.75	-0.124
Dfc	IT-Tor	GRA	YES	12	3.31	920	75.53	-0.147*
Dfc	CH-Aws	GRA	YES	8	3.76	918	373.64	-0.076
Dfc	SE-Deg	WET	YES	20	2.57	523	53.96	0.065
Dfc	CH-Dav	ENF	NO	15	4.74	1062	83.56	-0.158**
Dfd	US-BZB	WET	NO	9	-1.55	274	-14.10	-0.051
Dfd	US-BZF	WET	NO	8	-1.13	274	-11.26	-0.039
Dwc	US-Uaf	ENF	YES	9	-3.16	263	43.44	-0.035
ET	US-ICt	OSH	NO	11	-5.48	318	2.68	-0.331**
ET	US-ICh	OSH	NO	11	-6.62	318	-14.82	-0.158**
ET	US-ICs	WET	NO	10	-6.54	318	-81.03	-0.077

Note: TRS_{ER} values marked with “*” and “**” denote statistically significant estimates at the 0.1 and 0.05 levels, respectively. The full names of climate class abbreviations are as follows: Am (tropical monsoon climate), Bsh (hot semi-arid climate), Bsk (cold semi-arid climate), Bwk (cold desert climate), Cfa (humid subtropical climate), Cfb (temperature oceanic climate), Csa (hot-summer Mediterranean climate), Csb (warm-summer Mediterranean climate), Dfa (hot-summer humid continental climate), Dfb (warm-summer humid continental climate), Dfc (subarctic climate), Dfd (extremely cold subarctic climate), Dwc (monsoon-influenced subarctic climate), and ET (tundra climate). We used the climate classifications reported by the AmeriFlux and FLUXNET websites for most sites, except for two sites: CA-LP1 (changed from Csa to Dfb) and US-MtB (changed from Dwb to Csb). These changes were made due to the inconsistency between the reported climate classifications and local climate conditions[86]. The full names of vegetation class abbreviations are as follows: DBF (deciduous broadleaf forests), EBF (evergreen broadleaf forests), ENF (evergreen needleleaf forests), MF (mixed forests), CSH (closed shrublands), OSH (open shrublands), SAV (savannas), WSA (woody savannas), GRA (grasslands), and WET (permanent wetlands).

Table S2. Thermal response strength (*TRS*) of leaf, root, and soil respirations estimated from *in-situ* warming experiments and field-measured data that exhibited significant compensating thermal responses (i.e., thermal acclimation and negative *TRS*) in the literature.

Respiration type	Vegetation class	*TRS* (1/℃)	Warming experiment/ seasonal measurement	Data sources
soil	evergreen needleleaf forests	-0.160	warming experiment	Strömgren et al., 2001[87]
soil	grasslands	-0.081	warming experiment	Luo et al., 2001[26]
leaf	deciduous broadleaf forests	-0.062	seasonal measurement	Bolstad et al., 2003[34]
leaf	evergreen broadleaf forests	-0.106	warming experiment	Bruhn et al., 2007[88]
leaf	multiple biome	-0.034	seasonal measurement	Zhu et al., 2021[57]
leaf	grasslands	-0.188	warming experiment	Chi et al., 2013[89]
leaf	deciduous broadleaf forests	-0.090	seasonal measurement	Lee et al., 2005[90]
leaf	deciduous broadleaf forests	-0.070	seasonal measurement	Lee et al., 2005[90]
leaf	deciduous broadleaf forests	-0.053	seasonal measurement	Lee et al., 2005[90]
leaf	evergreen needleleaf forests	-0.086	seasonal measurement	OW et al., 2010[91]
leaf	deciduous broadleaf forests	-0.035	seasonal measurement	OW et al., 2010[91]
leaf	deciduous broadleaf forests	-0.085	seasonal measurement	Rodríguez-Calcerrada et al., 2009[92]
leaf	deciduous broadleaf forests	-0.095	seasonal measurement	Rodríguez-Calcerrada et al., 2009[92]
leaf	deciduous broadleaf forests	-0.093	seasonal measurement	Rodríguez-Calcerrada et al., 2009[92]

leaf	grasslands	-0.158	seasonal measurement	Searle et al., 2011[93]
leaf	grasslands	-0.247	seasonal measurement	Searle et al., 2011[93]
leaf	evergreen needleleaf forests	-0.068	warming experiment	Reich et al., 2016[61]
leaf	evergreen needleleaf forests	-0.064	warming experiment	Reich et al., 2016[61]
leaf	evergreen needleleaf forests	-0.027	warming experiment	Reich et al., 2016[61]
leaf	evergreen needleleaf forests	-0.022	warming experiment	Reich et al., 2016[61]
leaf	evergreen needleleaf forests	-0.057	warming experiment	Reich et al., 2016[61]
leaf	deciduous broadleaf forests	-0.058	warming experiment	Reich et al., 2016[61]
leaf	deciduous broadleaf forests	-0.026	warming experiment	Reich et al., 2016[61]
leaf	deciduous broadleaf forests	-0.045	warming experiment	Reich et al., 2016[61]
leaf	deciduous broadleaf forests	-0.064	warming experiment	Reich et al., 2016[61]
leaf	deciduous broadleaf forests	-0.030	warming experiment	Reich et al., 2016[61]
leaf	evergreen needleleaf forests	-0.069	seasonal measurement	Reich et al., 2016[61]
leaf	deciduous broadleaf forests	-0.039	seasonal measurement	Reich et al., 2016[61]
soil	shrub	-0.503	warming experiment	Rousk et al., 2013[94]
soil	shrub	-0.072	warming experiment	Rousk et al., 2014[94]
soil	grasslands	-0.051	warming experiment	Shen et al., 2020[95]

soil	grasslands	-0.223	warming experiment	Zhang et al., 2013[96]
soil	grasslands	-0.346	warming experiment	Suzuki et al., 2016[97]
soil	grasslands	-0.240	warming experiment	Suzuki et al., 2016[97]
soil	grasslands	-0.389	warming experiment	Zhao et al., 2019[98]
soil	grasslands	-0.150	warming experiment	Chen et al., 2016[99]
soil	grasslands	-0.173	warming experiment	Wang et al., 2019[100]
soil	grasslands	-0.109	warming experiment	Wang et al., 2019[100]
soil	mixed forests	-0.144	warming experiment	Suseela et al., 2013[24]
soil	mixed forests	-0.090	warming experiment	Suseela et al., 2013[24]
soil	mixed forests	-0.080	warming experiment	Suseela et al., 2013[24]
root	evergreen needleleaf seedlings	-0.085	warming experiment	Chen et al., 2021[30]
root	evergreen needleleaf seedlings	-0.044	warming experiment	Chen et al., 2021[30]
root	evergreen needleleaf seedlings	-0.169	warming experiment	Jiang et al., 2023[101]

Note: “seasonal measurement” refers to the method of measuring respiration at a set temperature multiple times in the field, across different growth temperature. The mean set-temperature respiration rate across all the measurements served as the control condition, with each individual measurement treated as a treatment condition. Equation (4) was used to calculate *TRS* for studies using this method. For warming experimental studies, Equations (1-2) were used to calculate *TRS*. We only selected studies that demonstrated significant thermal acclimation, most of which provided sufficient data for *TRS* estimation. Studies reporting non-

significant or enhancing thermal responses were excluded because most of them lacked adequate respiration data to calculate *TRS*. Although a few of these studies did provide enough data, their inclusion could introduce bias, as the limited number of such studies and omission of most studies with inadequate data would make direct comparisons with *TRS* estimates from this study unreliable.

Table S3. Geographic, climatic, soil, and vegetation variables potentially affecting thermal response strength in ecosystem respiration TRS_{ER}

Category	Variable name	Abbreviation	Description (unit)
Geography	Elevation	ELEV*	Elevation (m)
Climate	Mean precipitation	MAP	The mean total annual precipitation (mm)
	Mean temperature	MAT*	The mean annual air temperature (℃)
	Temperature seasonality	SST	The mean intra-annual standard deviation of daily air temperature (unitless)
	Temperature daily range	DRT	The average of air temperature range within a day (℃)
	Temperature interannual variation	IAT	The interannual standard deviation of annual mean air temperature (unitless)
Soil	Soil carbon content	SOC*	Soil organic carbon stocks of the top 0.3 m soils (t ha^{-1})
Vegetation	Normalized difference vegetation index	NDVI	The mean annual normalized difference vegetation index (unitless), calculated using remotely sensed data
	Enhanced vegetation index	EVI	The mean annual Landsat enhanced vegetation index (unitless), calculated using remotely sensed data
	Leaf area index	LAI*	The mean annual leaf area index (m^2 m^{-2}), calculated using remotely sensed data
	Gross primary productivity	GPP	The mean annual gross primary productivity (kg C m^{-2} yr^{-1}), calculated using remotely sensed data, as some sites do not have partitioned GPP data.

Note: the variables with “*” are selected representative variables for the random forest model to analyze how TRS_{ER} varies with each of them.

Table S4. The climate-specific thermal response strength in ecosystem respiration (TRS_{ER}) and its effects on mediating future increase in ecosystem respiration (ER)

The Köppen climate class	TRS_{ER} ($°C^{-1}$) Mean ± sd	Change in future ER by 2041-2060 (%)		
		"No thermal response"	"All thermal responses"	"Significant thermal responses"
Tropical monsoon (Am, *n*=1)	-0.164	3.3	0.0	0.0
Hot semi-arid (Bsh, *n*=2)	-0.139 ± 0.115	6.5 ± 4.8	1.9 ± 2.6	1.9 ± 2.6
Cold semi-arid (Bsk, *n*=4)	-0.071 ± 0.077	6.8 ± 0.5	3.4 ± 6.9	5.1 ± 3.5
Cold desert (Bwk, *n*=1)	-0.006	6.2	5.5	6.2
Humid subtropical (Cfa, n=7)	-0.074 ± 0.033	7.0 ± 2.9	0.3 ± 0.9	4.0 ± 3.9
Temperature oceanic (Cfb, *n*=14)	-0.057 ± 0.081	7.5 ± 5.5	5.6 ± 6.3	5.5 ± 6.5
Hot-summer Mediterranean (Csa, *n*=10)	-0.003 ± 0.051	4.1 ± 2.7	5.1 ± 4.9	4.1 ± 2.7
Warm-summer Mediterranean (Csb, *n*=4)	-0.151 ± 0.138	4.1 ± 9.5	0.0 ± 0.0	-0.6 ± 6.0
Hot-summer humid continental (Dfa, *n*=6)	-0.057 ± 0.021	11.7 ± 4.3	3.3 ± 3.9	9.0 ± 6.7
Warm-summer humid continental (Dfb, *n*=25)	-0.060 ± 0.085	11.8 ± 5.4	7.4 ± 8.4	9.7 ± 7.3
Subarctic (Dfc, *n*=13)	-0.062 ± 0.067	19.9 ± 7.2	11.3 ± 11.3	13.1 ± 10.2
Extremely cold subarctic (Dfd, *n*=2)	-0.045 ± 0.009	7.1 ± 2.6	2.4 ± 3.3	7.1 ± 2.6
Monsoon-influenced subarctic (Dwc, *n*=1)	-0.035	11.4	5.8	11.4
Tundra (ET, *n*=3)	-0.189 ± 0.130	18.8 ± 5.4	3.4 ± 5.9	6.0 ± 10.3

References

1. Keenan, T. F. & Williams, C. A. The terrestrial carbon sink. *Annu Rev Environ Resour* **43**, 219–243 (2018).
2. Ruehr, S. *et al.* Evidence and attribution of the enhanced land carbon sink. *Nat Rev Earth Environ* **4**, 518–534 (2023).
3. Buma, B. *et al.* Expert review of the science underlying nature-based climate solutions. *Nat Clim Chang* **14**, 402–406 (2024).
4. Zhu, Z. *et al.* Greening of the Earth and its drivers. *Nat Clim Chang* **6**, 791–795 (2016).
5. Wang, S. *et al.* Recent global decline of CO2 fertilization effects on vegetation photosynthesis. *Science (1979)* **370**, 1295–1300 (2020).
6. Zhao, M. & Running, S. W. Drought-induced reduction in global terrestrial net primary production from 2000 through 2009. *Science (1979)* **329**, 940–943 (2010).
7. Peñuelas, J. *et al.* Shifting from a fertilization-dominated to a warming-dominated period. *Nature Ecology and Evolution* vol. 1 1438–1445 Preprint at https://doi.org/10.1038/s41559-017-0274-8 (2017).
8. Bond-Lamberty, B., Bailey, V. L., Chen, M., Gough, C. M. & Vargas, R. Globally rising soil heterotrophic respiration over recent decades. *Nature* **560**, 80–83 (2018).
9. Carey, J. C. *et al.* Temperature response of soil respiration largely unaltered with experimental warming. *Proc Natl Acad Sci U S A* **113**, 13797–13802 (2016).
10. Sun, W. *et al.* Biome-scale temperature sensitivity of ecosystem respiration revealed by atmospheric CO2 observations. *Nat Ecol Evol* **7**, 1199–1210 (2023).
11. Yu, P. *et al.* Global pattern of ecosystem respiration tendencies and its implications on terrestrial carbon sink potential. *Earths Future* **10**, (2022).
12. Bradford, M. A. *et al.* Cross-biome patterns in soil microbial respiration predictable from evolutionary theory on thermal adaptation. *Nat Ecol Evol* **3**, 223–231 (2019).
13. Lombardozzi, D. L., Bonan, G. B., Smith, N. G., Dukes, J. S. & Fisher, R. A. Temperature acclimation of photosynthesis and respiration: A key

uncertainty in the carbon cycle-climate feedback. *Geophys Res Lett* **42**, 8624–8631 (2015).

14. Smith, N. G. & Dukes, J. S. Plant respiration and photosynthesis in global-scale models: Incorporating acclimation to temperature and CO2. *Glob Chang Biol* **19**, 45–63 (2013).
15. Bradford, M. A. *et al.* Thermal adaptation of soil microbial respiration to elevated temperature. *Ecol Lett* **11**, 1316–1327 (2008).
16. Atkin, O. K. & Tjoelker, M. G. Thermal acclimation and the dynamic response of plant respiration to temperature. *Trends in Plant Science* vol. 8 343–351 Preprint at https://doi.org/10.1016/S1360-1385(03)00136-5 (2003).
17. Bradford, M. A. Thermal adaptation of decomposer communities in warming soils. *Frontiers in Microbiology* vol. 4 Preprint at https://doi.org/10.3389/fmicb.2013.00333 (2013).
18. Karhu, K. *et al.* Temperature sensitivity of soil respiration rates enhanced by microbial community response. *Nature* **513**, 81–84 (2014).
19. Metze, D. *et al.* Soil warming increases the number of growing bacterial taxa but not their growth rates. *Sci Adv* **10**, 6295 (2024).
20. Nie, M. *et al.* Positive climate feedbacks of soil microbial communities in a semi-arid grassland. *Ecol Lett* **16**, 234–241 (2013).
21. He, Y. *et al.* Apparent thermal acclimation of soil heterotrophic respiration mainly mediated by substrate availability. *Glob Chang Biol* **29**, 1178–1187 (2023).
22. Liu, W., Zhang, Z. & Wan, S. Predominant role of water in regulating soil and microbial respiration and their responses to climate change in a semiarid grassland. *Glob Chang Biol* **15**, 184–195 (2009).
23. Michaletz, S. T., Cheng, D., Kerkhoff, A. J. & Enquist, B. J. Convergence of terrestrial plant production across global climate gradients. *Nature* **512**, 39–43 (2014).
24. Suseela, V. & Dukes, J. S. The responses of soil and rhizosphere respiration to simulated climatic changes vary by season. *Ecology* **94**, 403–413 (2013).
25. Niu, B. *et al.* Warming homogenizes apparent temperature sensitivity of ecosystem respiration. *Sci Adv* **7**, (2021).

26. Luo, Y., Wan, S., Hui, D. & Wallace, L. L. Acclimatization of soil respiration to warming in a tall grass prairie. *Nature* **413**, 622–625 (2001).

27. Vanderwel, M. C. *et al.* Global convergence in leaf respiration from estimates of thermal acclimation across time and space. *New Phytologist* **207**, 1026–1037 (2015).

28. Slot, M. & Kitajima, K. General patterns of acclimation of leaf respiration to elevated temperatures across biomes and plant types. *Oecologia* **177**, 885–900 (2015).

29. Loveys, B. R. *et al.* Thermal acclimation of leaf and root respiration: an investigation comparing inherently fast-and slow-growing plant species. *Glob Chang Biol* **9**, 895–910 (2003).

30. Chen, T. *et al.* Does root respiration of subtropical Chinese fir seedlings acclimate to seasonal temperature variation or experimental soil warming? *Agric For Meteorol* **308**, 108612 (2021).

31. Dacal, M., Bradford, M. A., Plaza, C., Maestre, F. T. & García-Palacios, P. Soil microbial respiration adapts to ambient temperature in global drylands. *Nat Ecol Evol* **3**, 232–238 (2019).

32. Zhu, L. *et al.* Acclimation of leaf respiration temperature responses across thermally contrasting biomes. *New Phytologist* **229**, 1312–1325 (2021).

33. Reich, P. B. *et al.* Boreal and temperate trees show strong acclimation of respiration to warming. *Nature* **531**, 633–636 (2016).

34. Bolstad, P. V, Reich, P. & Lee, T. Rapid temperature acclimation of leaf respiration rates in Quercus alba and Quercus rubra. *Tree Physiol* **23**, 969–976 (2003).

35. Crous, K. Y., Uddling, J. & De Kauwe, M. G. Temperature responses of photosynthesis and respiration in evergreen trees from boreal to tropical latitudes. *New Phytologist* vol. 234 353–374 Preprint at https://doi.org/10.1111/nph.17951 (2022).

36. Zhou, X., Liu, X., Wallace, L. L. & Luo, Y. Photosynthetic and respiratory acclimation to experimental warming for four species in a tallgrass prairie ecosystem. *J Integr Plant Biol* **49**, 270–281 (2007).

37. Hartley, I. P., Hopkins, D. W., Garnett, M. H., Sommerkorn, M. & Wookey, P. A. Soil microbial respiration in arctic soil does not acclimate to temperature. *Ecol Lett* **11**, 1092–1100 (2008).

38. Janzen, D. H. Why mountain passes are higher in the tropics. *Am Nat* **101**, 233–249 (1967).

39. Billings, W. D., Godfrey, P. J., Chabot, B. F. & Bourque, D. P. Metabolic acclimation to temperature in arctic and alpine ecotypes of Oxyria Digyna. *Arctic and Alpine Research* **3**, 277–289 (1971).

40. Tjoelker, M. G., Oleksyn, J., Lorenc-Plucinska, G. & Reich, P. B. Acclimation of respiratory temperature responses in northern and southern populations of Pinus banksiana. *New Phytologist* **181**, 218–229 (2009).

41. Strickland, M. S., Devore, J. L., Maerz, J. C. & Bradford, M. A. Grass invasion of a hardwood forest is associated with declines in belowground carbon pools. *Glob Chang Biol* **16**, 1338–1350 (2010).

42. Pielke, R. A. *et al.* Land use/land cover changes and climate: Modeling analysis and observational evidence. *Wiley Interdisciplinary Reviews: Climate Change* vol. 2 828–850 Preprint at https://doi.org/10.1002/wcc.144 (2011).

43. Crowther, T. W. & Bradford, M. A. Thermal acclimation in widespread heterotrophic soil microbes. *Ecol Lett* **16**, 469–477 (2013).

44. Karhu, K. *et al.* Temperature sensitivity of soil respiration rates enhanced by microbial community response. *Nature* **513**, 81–84 (2014).

45. Remkes, C. *et al.* Global convergence in the temperature sensitivity of respiration at ecosystem Level. *Science (1979)* **329**, 838–841 (2010).

46. Blagodatskaya, E., Blagodatsky, S., Khomyakov, N., Myachina, O. & Kuzyakov, Y. Temperature sensitivity and enzymatic mechanisms of soil organic matter decomposition along an altitudinal gradient on Mount Kilimanjaro. *Sci Rep* **6**, (2016).

47. BILLINGS, W. D. & MOONEY, H. A. The ecology of arctic and alpine plants. *Biological Reviews* **43**, 481–529 (1968).

48. Schimel, J., Balser, T. C. & Wallenstein, M. Microbial stress-response physiology and its implications for ecosystem function. *Ecology* vol. 88 1386–1394 Preprint at https://doi.org/10.1890/06-0219 (2007).

49. De Nadal, E., Ammerer, G. & Posas, F. Controlling gene expression in response to stress. *Nature Reviews Genetics* vol. 12 833–845 Preprint at https://doi.org/10.1038/nrg3055 (2011).

50. Pinkard, E. A., Eyles, A. & O'Grady, A. P. Are gas exchange responses to resource limitation and defoliation linked to source: Sink relationships? *Plant Cell Environ* **34**, 1652–1665 (2011).

51. Schimel, J. P. Life in dry soils: effects of drought on soil microbial communities and processes. *Annu Rev Ecol Evol Syst* **49**, 409–432 (2018).

52. Lecomte, S. M. *et al.* Diversifying anaerobic respiration strategies to compete in the rhizosphere. *Front Environ Sci* **6**, 139 (2018).

53. Allison, S. D., Wallenstein, M. D. & Bradford, M. A. Soil-carbon response to warming dependent on microbial physiology. *Nat Geosci* **3**, 336–340 (2010).

54. Fang, H., Baret, F., Plummer, S. & Schaepman-Strub, G. An overview of global leaf area index (LAI): Methods, products, validation, and applications. *Reviews of Geophysics* vol. 57 739–799 Preprint at https://doi.org/10.1029/2018RG000608 (2019).

55. Chieppa, J. *et al.* Thermal acclimation of leaf respiration is consistent in tropical and subtropical populations of two mangrove species. *J Exp Bot* **74**, 3174–3187 (2023).

56. Crous, K. Y. *et al.* Similar patterns of leaf temperatures and thermal acclimation to warming in temperate and tropical tree canopies. *Tree Physiol* **43**, 1383–1399 (2023).

57. Zhu, L. *et al.* Acclimation of leaf respiration temperature responses across thermally contrasting biomes. *New Phytologist* **229**, 1312–1325 (2021).

58. Piao, S. *et al.* Forest annual carbon cost: A global-scale analysis of autotrophic respiration. *Ecology* **91**, 652–661 (2010).

59. Kreft, H. & Jetz, W. Global patterns and determinants of vascular plant diversity. *Proc Natl Acad Sci U S A* **104**, 5925–5930 (2007).

60. Oliver, T. H. *et al.* Biodiversity and resilience of ecosystem functions. *Trends in Ecology and Evolution* vol. 30 673–684 Preprint at https://doi.org/10.1016/j.tree.2015.08.009 (2015).

61. Reich, P. B. *et al.* Boreal and temperate trees show strong acclimation of respiration to warming. *Nature* **531**, 633–636 (2016).

62. Denissen, J. M. C. *et al.* Widespread shift from ecosystem energy to water limitation with climate change. *Nat Clim Chang* **12**, 677–684 (2022).

63. Tian, C. *et al.* Projections of changes in ecosystem productivity under 1.5 °C and 2 °C global warming. *Glob Planet Change* **205**, (2021).

64. Knauer, J. *et al.* Higher global gross primary productivity under future climate with more advanced representations of photosynthesis. *Sci Adv* **9**, (2023).

65. Schuur, E. A. G. *et al.* Climate change and the permafrost carbon feedback. *Nature* **520**, 171–179 (2015).

66. Baldocchi, D. D. How eddy covariance flux measurements have contributed to our understanding of Global Change Biology. *Global Change Biology* vol. 26 242–260 Preprint at https://doi.org/10.1111/gcb.14807 (2020).

67. Richardson, A. D. *et al.* Tracking vegetation phenology across diverse North American biomes using PhenoCam imagery. *Sci Data* **5**, 1–24 (2018).

68. Chen, W. *et al.* Evidence for widespread thermal optimality of ecosystem respiration. *Nat Ecol Evol* **7**, 1379–1387 (2023).

69. Alster, C. J. *et al.* Quantifying thermal adaptation of soil microbial respiration. *Nat Commun* **14**, (2023).

70. Körner, C., Möhl, P. & Hiltbrunner, E. Four ways to define the growing season. *Ecol Lett* **26**, 1277–1292 (2023).

71. Warm Winter 2020 Team, & ICOS Ecosystem Thematic Centre. (2022). Warm Winter 2020 ecosystem eddy covariance flux product for 73 stations in FLUXNET-Archive format—release 2022-1 (Version 1.0). ICOS Carbon Portal. https://doi.org/10.18160/2G60-ZHAK.

72. Tabachnick, B. G., Fidell, L. S. & Ullman, J. B. *Using Multivariate Statistics*. vol. 6 (Pearson Boston, MA, 2013).

73. Reichstein, M. *et al.* On the separation of net ecosystem exchange into assimilation and ecosystem respiration: Review and improved algorithm. *Global Change Biology* vol. 11 1424–1439 Preprint at https://doi.org/10.1111/j.1365-2486.2005.001002.x (2005).

74. Lee, S.-C. *et al.* Partitioning of net ecosystem exchange into photosynthesis and respiration using continuous stable isotope

measurements in a Pacific Northwest Douglas-fir forest ecosystem. *Agric For Meteorol* **292**, 108109 (2020).

75. Kira, O. *et al.* Partitioning net ecosystem exchange (NEE) of CO2 using solar-induced chlorophyll fluorescence (SIF). *Geophys Res Lett* **48**, e2020GL091247 (2021).
76. Keenan, T. F. *et al.* Widespread inhibition of daytime ecosystem respiration. *Nat Ecol Evol* **3**, 407–415 (2019).
77. Wutzler, T. *et al.* Basic and extensible post-processing of eddy covariance flux data with REddyProc. *Biogeosciences* **15**, 5015–5030 (2018).
78. Zhang, Q. *et al.* Water limitation regulates positive feedback of increased ecosystem respiration. *Nat Ecol Evol* (2024) doi:10.1038/s41559-024-02501-w.
79. Rastetter, E. B. *et al.* A general biogeochemical model describing the responses of the C and N cycles in terrestrial ecosystems to changes in CO2, climate, and N deposition. *Tree Physiol* **9**, 101–126 (1991).
80. Haaf, D., Six, J. & Doetterl, S. Global patterns of geo-ecological controls on the response of soil respiration to warming. *Nat Clim Chang* **11**, 623–627 (2021).
81. Crowther, T. W. *et al.* Quantifying global soil carbon losses in response to warming. *Nature* **540**, 104–108 (2016).
82. FAO & ITPS. *Global Soil Organic Carbon Map V1.5: Technical Report*. (2020).
83. Breiman, L., Cutler, A., Liaw, A. & Wiener, M. Package ‘randomforest’. *University of California, Berkeley: Berkeley, CA, USA* (2018).
84. Peng, S. *et al.* Asymmetric effects of daytime and night-time warming on Northern Hemisphere vegetation. *Nature* **501**, 88–92 (2013).
85. Liu, W., Allison, S. D., Xia, J., Liu, L. & Wan, S. Precipitation regime drives warming responses of microbial biomass and activity in temperate steppe soils. *Biol Fertil Soils* **52**, 469–477 (2016).
86. Beck, H. E. *et al.* High-resolution (1 km) Köppen-Geiger maps for 1901–2099 based on constrained CMIP6 projections. *Sci Data* **10**, 724 (2023).
87. Strömgren, M. *Soil-Surface CO2 Flux and Growth in a Boreal Norway Spruce Stand*. (Sveriges Lantbruksuniv., 2001).

88. Bruhn, D. A. N., Egerton, J. J. G., Loveys, B. R. & Ball, M. C. Evergreen leaf respiration acclimates to long-term nocturnal warming under field conditions. *Glob Chang Biol* **13**, 1216–1223 (2007).

89. Chi, Y. *et al.* Acclimation of foliar respiration and photosynthesis in response to experimental warming in a temperate steppe in northern China. *PLoS One* **8**, e56482 (2013).

90. Lee, T. D., Reich, P. B. & Bolstad, P. V. Acclimation of leaf respiration to temperature is rapid and related to specific leaf area, soluble sugars and leaf nitrogen across three temperate deciduous tree species. *Funct Ecol* 640–647 (2005).

91. Ow, L. F., Whitehead, D., Walcroft, A. S. & Turnbull, M. H. Seasonal variation in foliar carbon exchange in Pinus radiata and Populus deltoides: respiration acclimates fully to changes in temperature but photosynthesis does not. *Glob Chang Biol* **16**, 288–302 (2010).

92. Rodríguez-Calcerrada, J. *et al.* Thermal acclimation of leaf dark respiration of beech seedlings experiencing summer drought in high and low light environments. *Tree Physiol* **30**, 214–224 (2010).

93. Searle, S. Y. *et al.* Leaf respiration and alternative oxidase in field-grown alpine grasses respond to natural changes in temperature and light. *New phytologist* **189**, 1027–1039 (2011).

94. Rousk, J., Smith, A. R. & Jones, D. L. Investigating the long-term legacy of drought and warming on the soil microbial community across five European shrubland ecosystems. *Glob Chang Biol* **19**, 3872–3884 (2013).

95. Shen, R. *et al.* Microbial membranes related to the thermal acclimation of soil heterotrophic respiration in a temperate steppe in northern China. *Eur J Soil Sci* **71**, 484–494 (2020).

96. Zhang, N. *et al.* Soil microbial responses to warming and increased precipitation and their implications for ecosystem C cycling. *Oecologia* **173**, 1125–1142 (2013).

97. Suzuki, M. *et al.* Effects of long-term experimental warming on plants and soil microbes in a cool temperate semi-natural grassland in Japan. *Ecol Res* **31**, 957–962 (2016).

98. Zhao, J., Tian, L., Wei, H., Sun, F. & Li, R. Negative responses of ecosystem autotrophic and heterotrophic respiration to experimental

warming in a Tibetan semi-arid alpine steppe. *Catena (Amst)* **179**, 98–106 (2019).

99. Chen, J. I. *et al.* Differential responses of ecosystem respiration components to experimental warming in a meadow grassland on the Tibetan Plateau. *Agric For Meteorol* **220**, 21–29 (2016).

100. Wang, G. *et al.* Responses of soil respiration to experimental warming in an alpine steppe on the Tibetan Plateau. *Environmental Research Letters* **14**, 094015 (2019).

101. Jiang, Q. *et al.* Substrate and adenylate limit subtropical tree fine-root respiration under soil warming. *Plant Cell Environ* **46**, 2827–2840 (2023).

Supplementary Files

This is a list of supplementary files associated with this preprint. Click to download.

- Supplementaryinformation.docx